THE MONASTERY HILL: GEOPHYSICAL METHODS FOR DESCRIBING ARCHAEOLOGY AND NEAR-SURFACE GEOLOGY IN LÖDÖSE, SW SWEDEN

Tobias Möhl
Fredrik Andersson

Degree of Master of Science (120 credits)
with a major in Earth Sciences
45 hec

Department of Earth Sciences
University of Gothenburg
2021 B1159

Faculty of Science

UNIVERSITY OF GOTHENBURG

UNIVERSITY OF GOTHENBURG
Department of Earth Sciences
Geovetarcentrum/Earth Science Centre

THE MONASTERY HILL: GEOPHYSICAL METHODS FOR DESCRIBING ARCHAEOLOGY AND NEAR-SURFACE GEOLOGY IN LÖDÖSE, SW SWEDEN

Tobias Möhl
Fredrik Andersson

ISSN 1400-3821

B1159
Master of Science (120 credits) thesis
Göteborg 2021

Mailing address
Geovetarcentrum
S 405 30 Göteborg

Address
Geovetarcentrum
Guldhedsgatan 5A

Telephone
031-786 19 56

Geovetarcentrum
Göteborg University
S-405 30 Göteborg
SWEDEN

ABSTRACT

Even though Sweden has been one of the leading countries in the development of near-surface geophysics instrumentation and practices, geophysical surveys in archaeology are not commonly used in Sweden. However, it is becoming increasingly popular, especially the use of ground-penetrating radar and metal detectors. Therefore, it is of great interest to investigate the usability of other geophysical methods for accurately describing the archaeological potential. This study aims at comparing resistivity and magnetic gradiometry to previous ground-penetrating radar measurements and archaeological excavations. The study area is located in Lödöse, South-West Sweden, which was once one of the most important cities in medieval Sweden. The surveys were made over the Monastery Hill, where a Dominican monastery and an older church are located beneath the surface. This study is showing that clearer images are given from the GPR measurements, but additional features can be seen in the resistivity results. The magnetic gradiometry does not show any structures that can easily be compared to the GPR and resistivity but shows another structure that does not appear in the other two surveys. The resistivity and gradiometry surveys are also used to interpret the material of the archaeological features as well as the surrounding geology. All in all, the different methods have different pros and cons and illuminate different archaeological features in the subsurface. Used together, they can give an unsurpassed information source, short of excavation only.

Key words: *Near-surface geophysics*, *Ground-penetrating radar*, *Resistivity*, *Magnetic gradiometry*, *3D modeling*, *Archaeology*, *Leached clay*, *Medieval monastery*, *Sweden*

ACKNOWLEDGEMENTS

Special thanks to our supervisors Prof. Erik Sturkell and Dr. Martin Persson who have shown a great interest in the topic of geophysics in archaeology and been of great help; Dr Tony Axelsson who have provided invaluable expertise with GPR measurements, data processing and interpretation; Anton Lazarides and colleagues at Lödöse Museum who taught us about the archaeological history of Lödöse; Andrea Håkansson who assisted with GPR measurements; Erik Wennerholm who provided his data from his study on the Monastery Hill; Martin Domeij and Stina Jarenskog, who live in the house on the Monastery Hill, who demonstrated great interest in the study and allowed us to do surveys on their private property; Jenny Wåhlander and Kyle Morris who corrected the language of the report and insured correct grammar; lastly, our examiner Dr. Mark Johnson who helped with perfecting the report before publication.

I (Tobias) would also like to acknowledge everyone who has accompanied me along this 5-year journey to become a geologist. The personal connection with the teachers at Geovetarcentrum is something that I treasure. The passion for their research topics and that they know the names of us students and what our interests are have made the education fun and valuable. I would also like to thank my family who has let me find and follow my path in life and supported me to be the person I want to be. Lastly, I want to thank my friends who have given me much laughter and happiness through all times in life and supported me in my interests.

CONTENTS

1 INTRODUCTION

This report is one part of a larger study that was done in two areas in Lödöse, Southwest Sweden. This report will focus on the Monastery Hill, where the subsurface ruins of a Dominican monastery and an older church preceding the monastery are located. The second part, the medieval castle Lödösehus, will be covered in Andersson & Möhl (2021). All data that was gathered, processed and interpreted in both papers has been done so in close collaboration.

1.1 Geophysics in archaeology

A question that always benefits from being answered by earth scientists or geotechnical engineers is what appears beneath the ground's surface. This is generally done by drilling, soundings or test pits, which can provide point data that can be combined into models. In some cases, there is a need to construct a full image covering all data points in the study area without disturbing the sediment (or at least to get data points between drill holes). This is where remote measurements like geophysics come in to map the subsurface (Musset & Khan, 2000, p. 4). There are several different tools used in geophysics that all have different applicability with their associated pros and cons.

The development of geophysical techniques and equipment often has its roots in oil and mineral exploration, but these have since been adapted to nearer-surface investigations in environmental and engineering surveys. For geophysics to work at its best, there is a need for a measurable contrast of the physical properties between different mediums. For this reason, geophysics is also used in archaeology, where sharp contrasts can often be found between archaeological findings and the surrounding sediment (Milsom & Eriksen, 2011, p. 1).

Despite Sweden being one of the leading countries in the development of near-surface geophysics, geophysical surveys are not commonly used in archaeology, perhaps with the exception of simple metal detectors. One reason for this is Sweden's geology and land cover. Approximately three quarters of the land surface is covered by forests and other wooded areas that generally prohibit effective measurements. Also, the Weichselian glaciation has left a surface cover of till and other glacial sediments. The combination of forests and unsorted, heterogeneous sediments has made it difficult to gather data of both quality and quantity. Further problems can occur where the depth to bedrock is shallow, which can affect the collected data, or where a thick layer of clay is present, that may limit the penetration depth of some surveys. Still, there are numerous archaeological sites in Sweden with promising geophysical survey conditions. Geophysics has previously most likely not been used due to bad initial experiences and tradition (Viberg et al., 2011). However, geophysics in Swedish archaeology is becoming more popular, especially the use of ground-penetrating radar (Rundkvist & Viberg, 2014).

This master thesis will hopefully shed light on the potential of geophysical surveying in archaeology. Since ground-penetrating radar has been of great success in Sweden in recent times (e.g. (Karlsson et al., 2014; Viberg & Wikström, 2014; Westergaard et al., 2019)), it is of interest to investigate if other geophysical instruments can be proved to be of use. The benefit of geophysical instruments are myriad: they are non-destructive, they can pinpoint areas, thus allowing archaeologists to know where to and where not to conduct an excavation, they can provide complementary information to excavations, and they can also find areas of interest that would otherwise remain undiscovered (Viberg et al., 2011). The use of geophysical surveys are also indirectly recommended by the Council of Europe. The Valletta Convention states that non-destructive methods of investigation should be applied wherever possible to protect the archaeological heritage (Council of Europe, 1992).

Three different geophysical methods will be used in this study: ground-penetrating radar, resistivity, and magnetic gradiometry. The geophysical aspects of the different tools will be tested by the archaeological objects. The key question is whether different instruments used over the same study area give overlapping results, or if a combination of methods can give a better joint interpretation of structures and materials. The contrast between the archaeological objects and the geology in the area may determine how the results will differ between methods. Known archaeological features mapped from previous excavations will be used as a guide to interpret and understand the geophysical data surveyed over areas not yet excavated.

1.2 Geological setting of Lödöse

Lödöse is located in the Göta river valley (Figure 1.1). The area was covered by kilometers of ice during the last glaciation. The ice started to retreat from the Gothenburg area around 14,500 years ago and the Göta river valley was completely ice free 2,000 years later (Klingberg et al., 2006). At this point the land started to rise owing to isostatic forces, but the valley was still under water with marine and archipelagic conditions. The water was calm with relatively weak currents since the valley was protected by a large island to the west. The salinity was high in the deep water, while the surface water was brackish. As the isostatic rebound continued, the valley had 11,000 years ago become a strait between the main land and the large island in the west (Klingberg et al., 2006).

Thick layers of clay were deposited in the deeper water. Cohesive sediment layers 60-80 meters thick are commonly found in the Göta river valley (Fredén, 1986, p. 42). The depth to bedrock can be even deeper locally, for example south of Lödöse where the depth can be over 100 meters. The sediment mainly consists of glacial clay with post-glacial clay overlying it (p. 50). Gravel and pebbles can occur in the clay. These would be dropstones that have been deposited by melting icebergs (Klingberg et al., 2006). Non-cohesive sediment can also be found between the bedrock and the clay (Figure 1.3). This is the case in Lödöse, where a drill core from the construction of the old motorway measured 33 meters of cohesive sediment and 9 meters of non-cohesive sediment before reaching the bedrock (Fredén, 1986, p. 42). The bedrock consists of red granitic augen gneiss (p. 22). Fluvial sediments can be found around watercourses, like around the Gårda stream that flows through

Lödöse. They consist of alternating layers of clay, silt and sand as well as gyttja with thin layers of organic content. The thickness is usually around 1 meter (p. 52).

As the isostatic rebound continued, the strait became a bay around 10,000 years ago when lake Vänern became disconnected from the ocean (Klingberg et al., 2006). As time went on, a river started to form (the Göta river), forming deltas as the mouth of the river shifted to the south. The clay particles flocculated in contact with the saline water, leading to a relatively fast sedimentation. The ground in Lödöse is therefore believed to have been a fine-grained delta with its flat plains of clay. While isostatic rebound is still occurring in Scandinavia, the Göta river valley has looked more or less the same for the last 2,000 years (Klingberg et al., 2006).

Figure 1.1: Overview map of the localities mentioned in this report. The study area is located in Lödöse. Bohus Fortress is also included on the map, which was an important fortification in medieval times.

Geological maps of Lödöse containing the different sediment types and the depth to bedrock are provided in Figure 1.2a and 1.2b. The maps contain the study area of the Monastery Hill as well as the study area Lödösehus that was surveyed in connection to this study (Andersson & Möhl, 2021). According to these maps, the sediment by the Monastery Hill is of post-glacial clay and some gyttja clay. The depth to bedrock is 20-30 meters. It is important point out that the map of the depth to bedrock is an interpolated model based on point observations, seen as the black triangles on the map. No observation has been made close to the Monastery Hill. The depth to bedrock must therefore be seen as approximate.

A common stratigraphy in the Gothenburg area can be seen in Figure 1.3 (Stevens et al., 1991). This is a generalization. Not all localities share the same features, but most areas have been affected and evolved in similar ways by the deglaciation. This figure is therefore a suitable representation of the geology in Lödöse. Just as described above, the figure shows the bottom layer to be non-cohesive sediment (diamicton and sand) and cohesive sediment layers (clay and silt) of different kinds overlaying it. Sand lenses can occur between the clay layers. High organic content can be found in the uppermost layers (post-glacial clay or gyttja) as well as sandy layers.

Added to Figure 1.2a is the water level of the Göta river in the late 13^{th} century, demonstrated by the diagonal lines. The water level was higher than it is today, partly because of the land rise due to isostatic forces, and partly because the outflow from Lake Vänern is controlled today, affecting the water level in the river (Åström et al., 2011). Moats were built around the castle Lödösehus as a fortification. They were connected to the Göta river as seen in the map. The Gårda stream was in the past called Ljuda stream and consisted of two branches, one northern and one southern, that surrounded the inner city, as seen as the dashed lines. The southern branch flowed closer to Lödösehus and acted as a natural moat. The northern branch of the Ljuda stream explains why floodplain sediment is found around the area of the beginning of that branch.

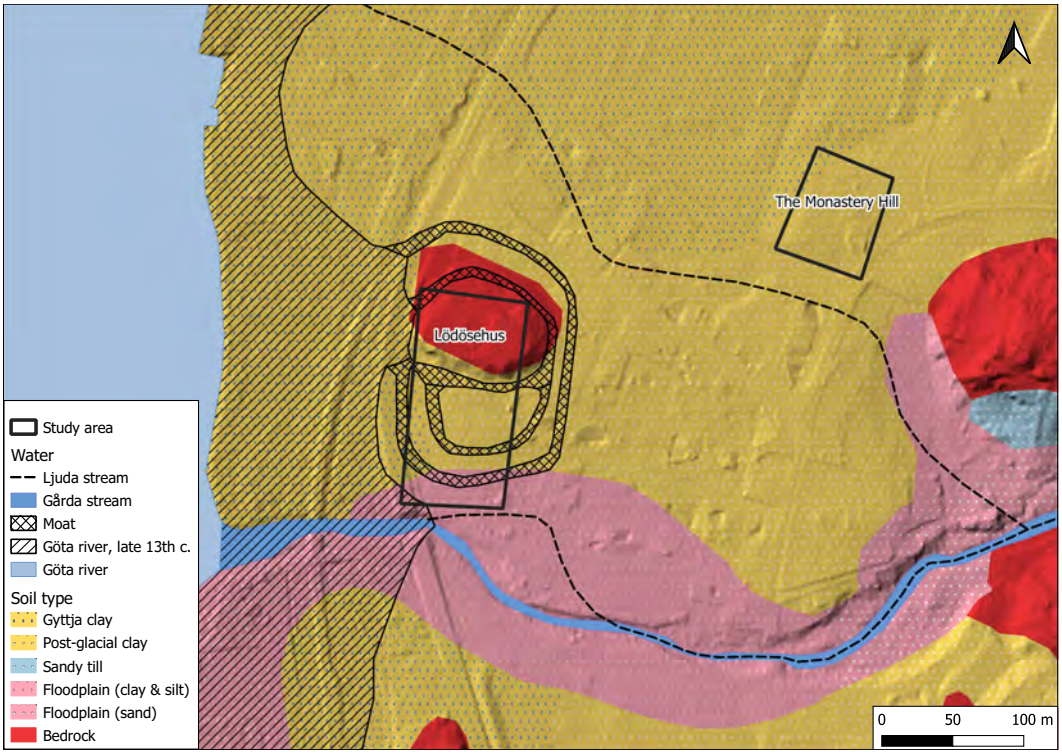

(a)

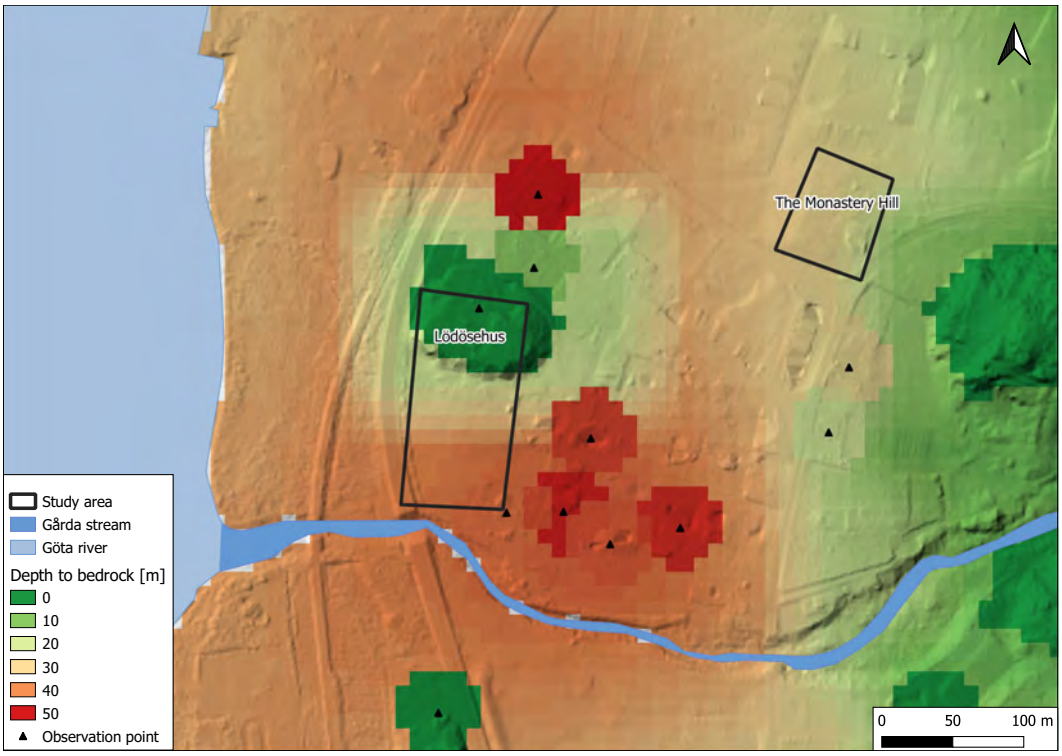

(b)

Figure 1.2: The study area in this thesis is marked as The Monastery Hill. The study area marked as Lödösehus is presented in Andersson & Möhl (2021). (a) Map of the sediment types in Lödöse (© Lantmäteriet; SGU) together with water levels and old streams and moats from the 13th century (Ekre, 2007, p. 109). (b) Map showing a model of the depth to bedrock in Lödöse. © Lantmäteriet; SGU

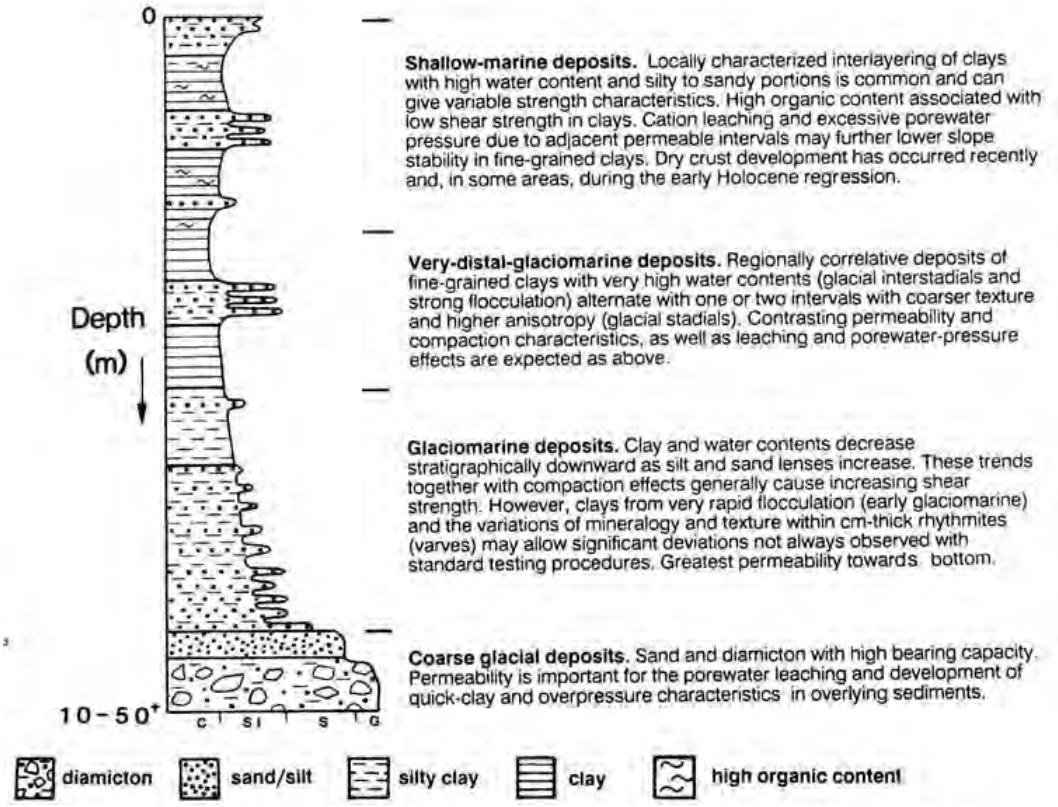

Figure 1.3: Common stratigraphical features in the Gothenburg area (Stevens et al., 1991).

As mentioned above, clay layers are very common in the Göta river valley. Clay particles are thin and elongated and have a negative electrical charge. As the clay particles flocculate in salt water, they do so in units that create pore spaces that retain water (Sällfors, 2013). As the former marine environment becomes land due to the isostatic rebound, the groundwater and precipitation percolates through the sediments which leaches the salts from the clays. This weakens the structure of the units, increasing the sensitivity of the clay and can ultimately lead to the formation of quick clay (SGI, 2020). High sensitive clays are common in western Sweden and quick clay is present in many places along the Göta river (Fredén, 1986, p. 43). There have been ten landslides along the Gårda stream, east of Lödöse (SGU, 2021). One of them was a large landslide that happened in 1953, called the Guntorp landslide, which disrupted the railway services for two months (Fredén, 1986, p. 48). A clay with a sensitivity of 50 or higher is considered to be quick clay. The clay in the area of the Guntorp landslide has been measured to have a sensitivity of 400 (p. 43). No landslide has been documented in Lödöse though, but the risk level for a landslide along the Gårda stream near the Göta river is deemed to be moderate (using a scale of low - moderate - high). The risk of a landslide occurring away from the stream is low (SGI, 2012).

1.3 History of Lödöse

The name Lödöse stems from the stream flowing through it. The stream is today called the Gårda stream (Gårdaån), but during the medieval ages it was called the Ljuda stream (Ljudaån). Lödöse is located by the stream's estuary, and the old Swedish word for estuary is "os". Therefore, the name Lödöse is believed to come from Ljudas os, or Ljudas's estuary (af Ugglas, 1931, pp. 19–20).

Nowadays, Lödöse is a small urban area. However, it was once one of the most important cities in medieval Sweden. Situated by the Göta river (Figure 1.1), it was the kingdom's only connection to the open sea because at the time Bohuslän belonged to Norway and Halland to Denmark, which constitutes the west coast, until 1645 (af Ugglas, 1931, p. 21). The issue of when Lödöse was founded is disputed. It is mentioned as Ljodhus in old Icelandic texts, such as Njál's saga, which suggests that Lödöse already existed as a larger town in the early 11th century (p. 25). This is supported by archaeological findings that make a strong case for Lödöse being present and flourishing in the mid 11th century (Ekre, 2007, p. 110). However, af Ugglas (1931, pp. 27-30) believes it rose to prominence after the Norwegian town of Kungahälla fell in 1135. These circumstances gave Lödöse the opportunity to prosper and Sweden could strengthen its position in the area. In any case, the 12th century is considered the beginning of Lödöse's history, with three stone churches built, one in the north, one in the east and one in the west (Figure 1.4).

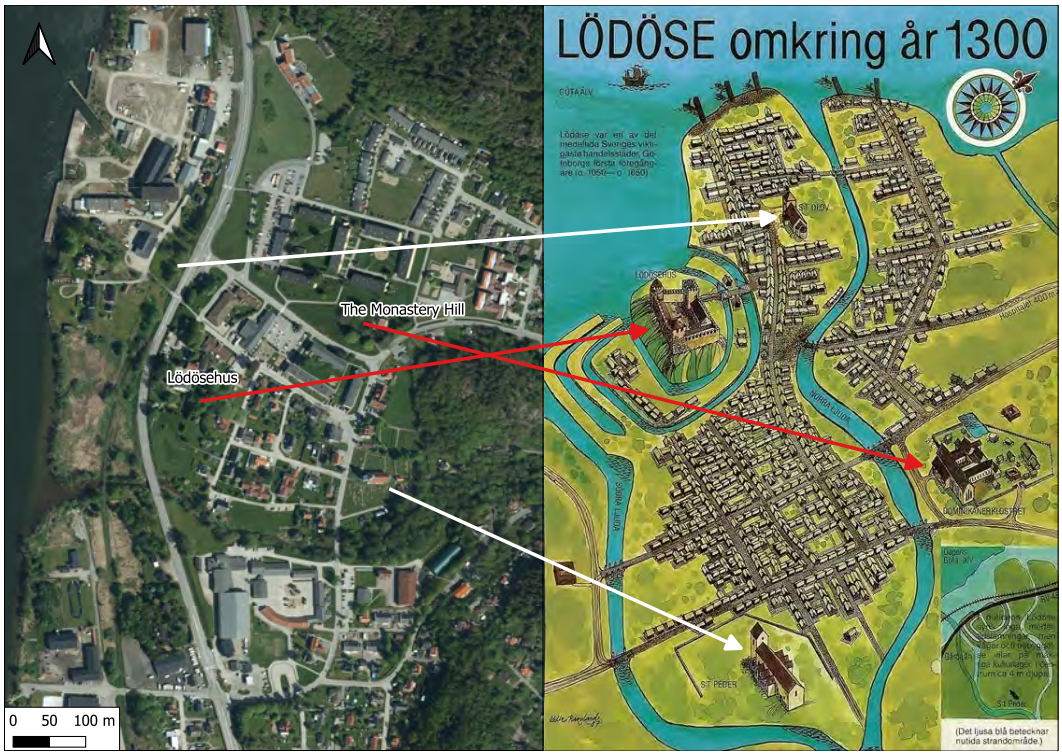

Figure 1.4: A comparison between an orthophoto (© Lantmäteriet) of Lödöse and an interpretation of Lödöse around year 1300 (© Lödöse Museum). The two study areas, the Monastery Hill and Lödösehus (described in Andersson & Möhl (2021)), are shown with red arrows. Two other churches, St. Peder (still in use, but rebuilt) and St. Olov (demolished), are shown with white arrows.

The archaeological discovery of a leather underlay for bracteate striking, along with dendrochronological dating from timber found in the same stratum, has established that Lödöse was a site of coin minting from the 1150s up until the 1360s. A bracteate is a single sided embossed coin. This makes Lödöse the earliest and most permanent site for the minting of coins in medieval mainland Sweden, in the kingdom only rivaled by Visby(?) on the island of Gotland (Ekre, 1991b, pp. 41, 47). A castellum was also built around the same time, which was later rebuilt in the 13th century as a castle named Lödösehus (Figure 1.4) (Carlsson, 1995, pp. 156–157). Lödöse was thus of great importance with a population of up to 2,000 people until year 1350 when the Black Death came and development came to a halt. Afterwards, the city had periods of both prosperity and hardships, before being destroyed by the Danes in 1453 (Ekre et al., 1994, p. 10). A large proportion of the population of Lödöse was instead moved in 1473 to New Lödöse, today's Old Town in Gothenburg (Figure 1.1). Lödöse however served as a military fortification all the way up to the 17th century (Ekre, 1991a, pp. 56–57).

1.3.1 The Monastery Hill

One locality that has been of great importance in the history of Lödöse was what is now called the Monastery Hill (our translation of *Klosterkullen*) (Figure 1.4). An archaeological investigation of this area was conducted between 1916-1920 by af Ugglas (1931). Only the southern part of the hill was excavated where the remains of two churches were found (excavation area in Figure 1.5). One of the churches was built on top of the other, indicating that it was one older and one younger church that had been found (af Ugglas, 1931, p. 216). As will be mentioned later in this report, it is known that the younger church was in fact part of a monastery and there are speculations that the older church might have been a part of a monastery as well.

There are no archaeological features visible on the surface today, except for the topography forming a hill in the study area. The only exposed object is a granitic stone wall located in the basement of the house on the hill (Figure 1.6A). Some rocks have however been placed on the ground to mark the extent of the monastery. Some of the walls close to the surface could also be felt when the metal rods from the resistivity survey was pushed into the ground.

Except for archaeological excavations done in 1964-1965 in the area surrounding the Monastery Hill (Figure 1.5), no investigations have been made since af Ugglas until recently. The Monastery Hill was studied between 2019-2020 by Wennerholm (2021) with various geophysical instruments as his master's thesis. One of the instruments used was a 3D ground-penetrating radar. A part of the results from his study is presented in Figure 1.7a. Here, the monastery can be seen with a church in the bottom of the image and a wall extending northward until it joins a wall going in an E-W direction. The same figure together with digitized, georeferenced maps of the older church (red colour) and the younger church (black colour) investigated by af Ugglas (1931) is shown in Figure 1.7b. Since there is a private property on the top of the hill, the monastery could not be surveyed with the GPR to its entirety.

The older church was built in stone with wooden flooring. The wall base, made of crystalline rocks, was built as cavity walls (a type of wall with a hollow center, filled with other material). Parts of the wooden floor have at some point been burnt (af Ugglas, 1931, pp. 216–222). It is not known

Figure 1.5: Approximate archaeological excavation areas conducted in 1916-1920 (grey) and 1964-1965 (light brown). Cable trench excavated in 1968 (yellow dashed line). (af Ugglas, 1931; Ekre, 1968). Orthophoto © Lantmäteriet

when the church was built, but the Romanesque architecture suggests that it was founded during the 12th century (Widéen, 1944, p. 313). This was the most vital century for monasteries in Nordic church history. It is still, however, up to debate whether this church also served a monastery. If it was part of a monastery, it might have belonged to the Premonstratensians (Ekre, 2007, pp. 125–127). The Premonstratensians, also called the Norbetines, are the fifth oldest Roman Catholic order in the world, founded in 1120 by St. Norbert of Xanten in Prémontré, France (Order of Prémontré, 2021).

The younger church, named St. Mary's Church, is of early Gothic architecture (Ekre, 2007, pp. 118–120). It is larger than the older church, but they share the northern wall with each other, and the southern wall has been straightened to be parallel to the northern wall (Figure 1.7b). The majority of the walls were built in stone to an height of 1.20 meters above floor level, and the remainder of the walls were built in brick. Both the stone walls and the brick walls were built as cavity walls filled with mortar and rocks (af Ugglas, 1931, p. 232). Two generations of a brick floor was found during af Ugglas's (1931) excavations. The older floor was made in a beautiful checkerboard pattern of green and yellow brick slabs, while the younger floor was less striking and made of regular bricks. The younger floor could be dated by a coin that was found in between the floors to around year 1520 (pp. 261-265). The northern wall of the younger church and the younger floor can be seen in Figure 1.6C.

By the two ends of the northern wall, there are connections to a cloister with herringbone brick flooring. The cloister was not investigated by af Ugglas (1931, p. 316), but the entrances to it gave evidence for St. Mary's Church to also serve as part of a monastery, meaning it was a residence for members of a religious community, in this case identified to be of the Dominican order (p. 209). The

Dominican order, also called the Order of the Preachers, was founded by St. Dominic de Guzman in 1216 when he saw a need for good Catholic preachers when travelling through Spain and southern France (Ordo Praedicatorum, 2021). The order grew quickly and already in 1243 was the Dominican monastery in Lödöse founded (af Ugglas, 1931, p. 209). The findings of the burnt wooden floor from the older church gives a clue to why this church monastery replaced the older church (p. 227), but not much evidence has been left about its history and its fate. It is likely that the Dominican monastery was demolished during the Protestant Reformation in the 1530s after another church in Lödöse was taken down by the order of King Gustav Vasa in 1528. The material from the churches was reused for other buildings and properties in Lödöse, but also in New Lödöse (Ekre, 2007, p. 154).

Figure 1.6: (A) The stone wall located in the basement of the house on the hill (Photo: T. Möhl). (B) The older dam (Ekre et al., 1994). (C) The northern wall of the younger church (af Ugglas, 1931).

An archaeological investigation of the areas west and north of the Dominican monastery (and a small area to the north-east) was conducted in 1964-1965 (Figure 1.5). The north-western corner of the cloister, the cemetery belonging to the church, streets, houses, a mint facility, a brick kiln, and two dams were found. One of the dams overlies the other, meaning that they are from different generations. The older dam (Figure 1.6B) has been dated to year 1085 +/- 100 years by carbon-14 dating of bottom material of the dam. Therefore, it might have existed at the same time as the older church. Adjacent to the older dam, a structure that is believed to have been a mill was found. The Premonstratensians were known to have farmed the land surrounding their monasteries. This mill is thus one argument for the older church to be a Premonstratensian monastery (Ekre, 2007, pp. 142–144).

(a)

(b)

Figure 1.7: (a) GPR image at 0.16 meters depth (Wennerholm, 2021), (b) with digitized georeferenced maps of the older (red) and younger (black) churches (af Ugglas, 1931). Orthophoto © Lantmäteriet

Ekre (2007, pp. 145-146) made sketches of how the Dominican monastery and the presumed Premonstratensian monastery could have looked like based on the excavations by af Ugglas in 1916-1920 and the excavations done in the 1964-1965. A digitized version of Dominican monastery can be seen georeferenced on top of a radar image from 0.16 meters depth in Figure 1.8a. Here is also an approximate location of a glassworks included. When a trench for a cable was excavated in 1968, east of the Dominican monastery (also seen in Figure 1.5), a part of another kiln was found together with glass slag. This means that a glassworks (a site where glass was made from raw materials) was a part of the Dominican monastery. It was the first medieval glassworks to be found in Sweden (Ekre, 2007, p. 149). The older church can be seen in Figure 1.8b georeferenced with a radar image from 1.60 meters depth. Schematic buildings are also placed on the map as how Ekre (2007) suggested that a Premonstratensian monastery could have looked like. It also includes the older dam and the mill.

(a)

Figure 1.8: (a) GPR image at 0.16 meters depth (Wennerholm, 2021), with digitized georeferenced map of the Dominican monastery (af Ugglas, 1931; Ekre, 2007). Cable location also included. Orthophoto © Lantmäteriet

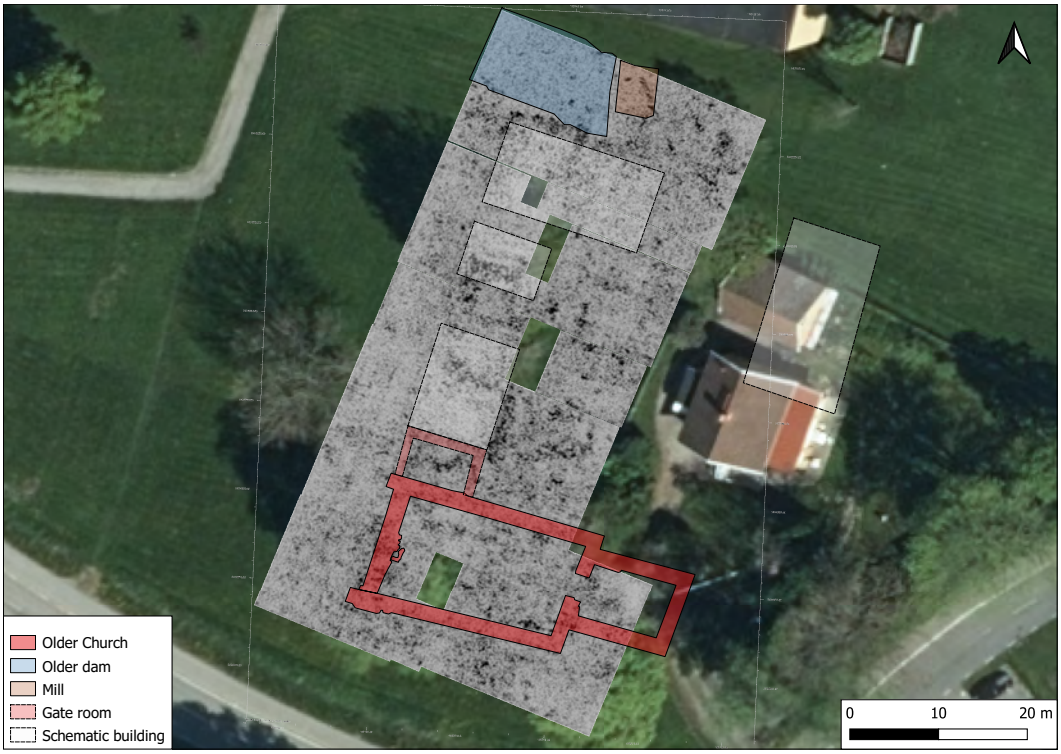

(b)

Figure 1.8: (b) GPR image at 1.60 meters depth (Wennerholm, 2021), with digitized geo-referenced map of buildings belonging to the Premonstratensian(?) monastery (af Ugglas, 1931; Ekre, 2007). Orthophoto © Lantmäteriet

The only Swedish Dominican church still in use is St. Mary's Church in Sigtuna (Figure 1.9). It is the best preserved Dominican church in the Nordic countries and it can be assumed that the church in Lödöse may have looked similar (Ekre, 2007, p. 130). St. Mary's Church in Sigtuna was founded in 1237 and served a monastery (af Ugglas, 1931, p. 210). However, the monastery buildings were, like in Lödöse, demolished around year 1530 (Storm, 2021).

Figure 1.9: St. Mary's Church in Sigtuna, Sweden.
Photo: Hans Hartman.

2 METHOD

2.1 GPR

The top few meters of ground are often the most important in archaeology, since it is here most archaeological features are found. The shallow depths are where ground-penetrating radar (GPR or radar for short) has great abilities to produce images in either 2D or 3D. This instrument has therefore become of great importance in archaeological surveys (Conyers, 2018, p. 18).

A GPR is an instrument with antennas that transmit and receive electromagnetic waves from the surface into the ground. The instruments come in different sizes dependent on the frequency of the antennas and the amount of antennas. The GPR used in this study is the MALÅ 3D Imaging Radar Array, also called MIRA (Figure 2.1). The same instrument was used by Wennerholm (2021). It is an 8-channel radar, with five transmitter and four receiver antennas at a frequency of 400 MHz. This radar can either be pulled directly on the ground, or be pushed like a cart by attaching wheels to its sides. Survey lines are made in straight profiles over the area of interest. A measuring wheel is attached to it that records the distance of the profiles. It also uses a Leica RTK GPS to set coordinates to the surveyed area. Every survey line produces a 2D profile. A screen is connected to the instrument which shows the result of the profile in real time. A preliminary result is thus given directly in the field. This allows the surveyor to know if the instrument is functional for the specific study area, or if settings need to be changed or if another frequency (if available) needs to be used. To acquire a 3D model of the study area, several profiles are made adjacent to each other. The profiles are then interpolated in a software program, producing a 3D model. The provided GPR data from Wennerholm (2021) was modeled in the software program rSlicer (DECO Geophysical, 2007-2010, Version 2.1.101001).

The waves transmitted from the GPR into the subsurface reflect on different interfaces as they propagate downwards. This can, for example, be at stratigraphic boundaries, buried objects or archaeological features. When the waves reach the surface, they are detected and recorded by a receiving antenna in the instrument. The receiving antenna measures the time between transmitting and receiving a wave. This is called the two-way travel time (TWT) and is measured in nanoseconds (ns) (Conyers, 2018, p. 19). If the geologic material is known, the TWT can be translated into meters, since the velocity of a wave is dependent on the medium it passes through (Musset & Khan, 2000, p. 229). Some radar waves will not be reflected back at interfaces but continue further down into the subsurface and be reflected from a deeper interface instead. This will continue until the energy finally dissipates and the signal is lost (Conyers, 2018, p. 19). The penetration depth is dependent on the frequency of the antennas and the conductivity of the material. The frequency also determines the resolution of the radar image. The resolution increases with higher frequency antennas but at a cost of

shallower penetration depth. Conversely, the penetration depth becomes deeper with low frequency antennas at a cost of lower resolution. The maximum depth however is not solely dependent on the instrument used but also on the properties of the subsurface. The radar energy decays rapidly in sediments with high conductivity. There are several factors that influence the conductivity of sediments, such as the degree of water saturation, but most importantly the concentration of dissolved salts. Wet sediments containing dissolved salts will have a higher signal attenuation. Clay, being a sediment that can have a high water saturation and contain salt, will therefore have a shallow penetration depth (Doolittle & Collins, 1995).

Figure 2.1: The MALÅ 3D Imaging Radar Array (MIRA) in use by F. Andersson for the Lödösehus survey (Andersson & Möhl, 2021).

2.1.1 Measurement and Processing

A GPR survey had already been done on the Monastery Hill by Wennerholm (2021). This data was obtained from him to be used as a guide to better interpret the data gathered in this study. The GPR data will therefore not be studied in detail but will be used in comparison to the resistivity and magnetic gradiometry surveys.

Different depth slices of the GPR data were imported to a geographic information system (GIS). The software program QGIS (QGIS Development Team, 2020, Version 3.10.12) was used. Since the radar images have coordinates attached to them, they were placed correctly on the map. Then other layers, such as the excavation maps (af Ugglas, 1931; Ekre, 2007), could be georeferenced to them.

To visualize the results and to aid interpretations, the noteworthy anomalies were digitized. The pixels in the radar images had colour values ranging from 0 to around 190, where the most prominent anomalies had values between 0 and 60. Contour lines were therefore made to circle all areas with a value of 60 or less. These lines were then converted to polygons. By doing this, anomalies from all depths could be shown at the same time.

2.2 Resistivity

By passing an electrical current through the ground, the subsurface can be investigated in what is called a resistivity survey. From a control unit, cables are laid out along a straight line. Electrodes are then connected to the cables and pushed into the ground. The current is passed through the electrodes into the subsurface and the variations in potential difference are measured, given hundreds to thousands available combinations of potential and current electrodes. This is given as resistivity (the inverse of conductivity), which has the unit ohm-meter (Ω-m) (Musset & Khan, 2000, pp. 181–183). The current does not take the shortest path between the electrodes but the easiest. It spreads out downwards and sideways, taking the path where the resistance is low. Most of the current will however be close to the surface (p. 185). The maximum penetration depth is partly dependent on the properties of the ground, but it is also determined by the distance between the outermost electrodes (p. 194). The larger the distance between the electrodes, the deeper the penetration, but with the cost of lower resolution. A higher resolution can be achieved with a shorter spacing of the electrodes, but then the penetration depth will be shallower (p. 198).

Resistivity surveys are often used for geological mapping, for example for finding quick clay, describing groundwater and potential ground contamination, or mineral prospecting, but also for other uses such as archaeological surveying. As long as there is a contrast in the resistivity of different materials, this method can be used (Musset & Khan, 2000, pp. 181–183). Typical resistivities of different geologic materials are shown in Figure 2.2. Note that crystalline rock may have much higher resistivity, for example granite can have a value of 1 million Ω-m (p. 183). Quick clay is also added to the figure to be distinguished from clay in general. The resistivity value of clay is mostly determined by its salt content. Since a quick clay has been leached from salt, the resistivity will be slightly higher than in a non-leached clay. In south-western Sweden, the lower limit has been set to 5 Ω-m (even though quick clay with lower resistivity does occur) (SGI, 2018). As was described in Chapter 1.2, the sediment in Lödöse has the potential to contain quick clay. It will be analysed if quick clay can be identified by the resistivity surveys. It will also be analyzed if the materials of the archaeological objects can be identified.

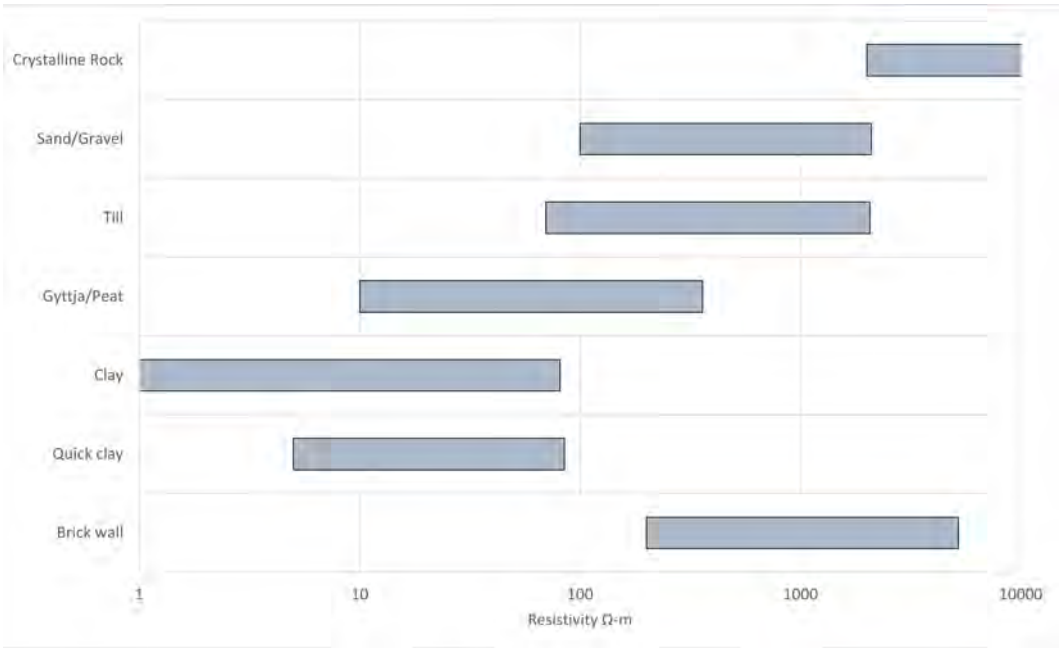

Figure 2.2: Typical resistivity values of different geologic materials and brick walls (De Donno et al., 2017; SGI, 2018; Triumf, 1992).

Important to mention about the resistivity of brick walls is that it may vary dependent on building technique and fractures. Laboratory experiments (De Donno et al., 2017) have shown that a heterogeneous undisturbed brick wall has a mean resistivity value of 700 Ω-m. A fracture in the wall can give resistivity values above 1000 Ω-m. Depending on building style, a more conductive brick wall can have a mean resistivity value as low as 300 Ω-m. It is the mortar in between the bricks that act as a conductive layer.

Not added to Figure 2.2 is the resistivity of cavities. The reason for this is because it is highly dependent on if it is filled with either air, water or loose materials, or a combination of the aforementioned. An air-filled cavity will result in a high resistivity value, whereas a water-filled cavity will have lower resistivity (Musset & Khan, 2000, p. 421). The acquired resistivity value is therefore highly circumstantial.

2.2.1 Measurement and Processing

Different instruments and different types of measurements can be used for resistivity surveying. In this study, the ABEM Terrameter LS was used (Figure 2.3). Three or four cables are usually connected to the instrument. Each cable has attachments for 21 electrodes, resulting in a profile length of 80 meters if four cables are used with an electrode spacing of 1 meter. Different arrays can be used with the Terrameter. In this study, the Gradient Plus array was used. This allows multiple measurements without the need to move the electrodes. Readings are automatically recorded using possible combinations of current and potential electrodes. Typically, roughly 848 data points will be stored for a four-cable array.

Figure 2.3: The ABEM Terrameter LS in use on the Monastery Hill.

A large part of the resistivity survey over the Monastery Hill had already been done by Wennerholm (2021). He made 26 profiles in a N-S direction, 60 meters long using three cables, with a distance of 1 meter apart from each other and with an electrode spacing of 1 meter. These profiles resulted in 2D images of the archaeological findings and the surrounding geology. The raw data of these profiles were obtained from Wennerholm to be constructed into 3D models. This was made in the software program Res2DInv (Geotomo Software, 2012, Version 3.59), where the resistivity profiles were collated into one 3D file. This file could then be opened in Res3DInv (Geotomo Software, 2007, Version 1.0; Geotomo Software), where it was processed. From Res3DInv, the data could be exported directly to the software program Voxler (Golder Software, LLC, 2019, Version 4.6.913). Where Res3DInv creates slices from different depths viewing the data from above, Voxler creates 3D models that can be rotated and viewed from all sides.

The resistivity profiles made by Wennerholm did not cover all of the Monastery Hill. The northernmost cloister wall was not included, and there is more of the hill that could be surveyed. Therefore, additional measurements were made. Seven profiles were made east of the house located in the study area. These were made to see if the wall in the basement of the house extended further to the east. The distance between the profiles was 1 meter and the electrode spacing was 0.5 meter, giving a profile length of 30 meters using three cables. As will be seen from the results from the magnetic gradiometry survey (Chapter 3.3), a large structure striking in an E-W direction is located in the northern part of the Monastery Hill which did not appear in the results from the initial resistivity survey by Wennerholm. More data was therefore acquired. A total of 25 profiles were made at the same location as the survey done by Wennerholm but starting 33 meters farther north. The distance between the profiles

was 1 meter and the electrode spacing was 0.5 meter. Four cables were used, giving a profile length of 40 meters. This survey also covered the northernmost cloister wall that was previously missed.

The data gathered in this study were processed in the same way as the data obtained from Wennerholm. The data described in the last paragraph was also combined with Wennerholm's data resulting in models where two data sets are interpolated with each other. Since the newly acquired data was made offset with a half meter relative to Wennerholm's, the resolution where they overlap became 0.5 meters between the profiles. The depth slices from Res3DInv could then be imported to QGIS by georeferencing the corners of the images to coordinates. The profiles were also analyzed in 2D, of which one will be presented in the results.

2.3 Magnetic Gradiometry

A magnetic gradiometer, or gradiometer for short, is an instrument suited to detect shallow objects in the ground. It is therefore often used in archaeological surveys (Musset & Khan, 2000, p. 176). A gradiometer is a variation of a magnetometer, both used for magnetic surveying. A magnetometer measures changes in the Earth's magnetic field. As for most geophysical instruments, different models can use different setups. The instrument used in this study was the GSM-19G from GEM Systems (Figure 2.4). To do a magnetic survey with this instrument, a sensor is mounted on top of a pole that measures the magnetic field in nano-Tesla (nT) (pp. 162-163). By adding an additional sensor to the pole, placed closer to the surface, the instrument becomes a gradiometer. This setup measures the gradient of the magnetic field between the sensors divided by the distance between them, and is given in nano-Tesla per meter (nT/m). This gradient (hence the name gradiometer) will be greater the closer a body is to the surface (p. 175). By measuring the difference between the upper and the lower sensor, the contribution of Earth's magnetic field is more or less eliminated since the reading of this value is essentially the same in both sensors. The measured values are therefore almost wholly a function of magnetic differences in the ground. This allows very weak magnetic variations produced by near-surface magnetic materials to be detectable (Conyers, 2018, p. 32).

Figure 2.4: The GSM-19G Gradiometer in use by T. Möhl on the Monastery Hill.

The measured data can be seen as anomalies that deviates negatively or positively from a value of zero. The anomalies will be a representation of how different materials vary magnetically as a function of how they modify the Earth's magnetic field. While the values of the anomalies can tell something about the composition of materials, it is the contrast between different materials, such as sediment, rock, and archaeological features, that are of importance. For example, if the soil is highly magnetic and the archaeological feature is of less susceptibility, the feature will have a negative anomaly. Reversely, if the soil is less magnetic than the archaeological feature, the feature will have a positive anomaly (Conyers, 2018, pp. 27–28). Most rocks have a lower susceptibility and remanence than soils. A stone wall will therefore likely have a negative anomaly (Musset & Khan, 2000, p. 430). Nearly all topsoils in the world are magnetically enriched. This means that any pit, ditch or other types of holes that have been refilled by topsoil will generate a positive anomaly. In some cases however, a previously positive anomaly can change into a negative anomaly. This can happen when a ditch filled with topsoil is exposed to a change in the groundwater table. A surplus of water may partly dissolve ferrimagnetic minerals and precipitate iron oxides, which will be seen as a negative anomaly in the data (Fassbinder, 2015).

2.3.1 Measurement and Processing

Over the Monastery Hill, 29 gradiometry profiles were made in a N-S direction with 1 meter spacing between measuring points. The length of the profiles was 65 meters. Three readings were made for each point from which the average value of these were used for processing. The profiles were made parallel to each other with a distance of 1 meter apart from each other, similar to the resistivity profiles. The profiles could have been longer, but disturbances from the building and perhaps subsurface cables to the north prohibited good readings to be acquired.

The data was first processed in Microsoft Excel (Microsoft 365MSO, Version 16.0) to obtain numerical data that could be imported to QGIS for further processing. Point data along the survey lines was created in QGIS containing the values from the gradiometry measurements. These points were interpolated using inversed distance weighting (IDW) with a resolution of 1 meter. It was then categorized into ten quantiles to give a good representation of the data.

3 RESULTS

3.1 GPR

As mentioned, the results from the GPR survey will not be presented in detail in this thesis, as it was covered by Wennerholm (2021). However, some of the results will be presented to make it easier to interpret the resistivity and the magnetic gradiometry surveys.

Figure 3.1 shows a radar image from a depth of 1.60 meters. The map also contain anomalies from every 5 centimeters in the GPR data between 1.05-1.75 meters depth. These anomalies will be used in the interpretations of the resistivity and the gradiometry data acquired in this study. The noteworthy anomalies are those forming quadrangular objects in the upper half of the radar image.

Figure 3.1: GPR image at 1.60 meters depth (Wennerholm, 2021) with overlying GPR anomalies (black) from 1.05-1.75 meters depth. Orthophoto © Lantmäteriet

3.2 Resistivity

The depth slice at 1.08-1.74 meters from the resistivity model made in Res3DInv using Wennerholm's data is georeferenced together with the digitized Dominican monastery buildings (af Ugglas, 1931; Ekre, 2007) in Figure 3.2. Here it can be seen which anomalies are shared with the monastery and how the resistivity profiles were too short to cover the cloister wall to the north. Low resistivity values are shown in blue to green colours and high values in yellow to red. The walls of the younger church are aligned well with the resistivity data. The cloister is not perfectly aligned, but similarities can be seen.

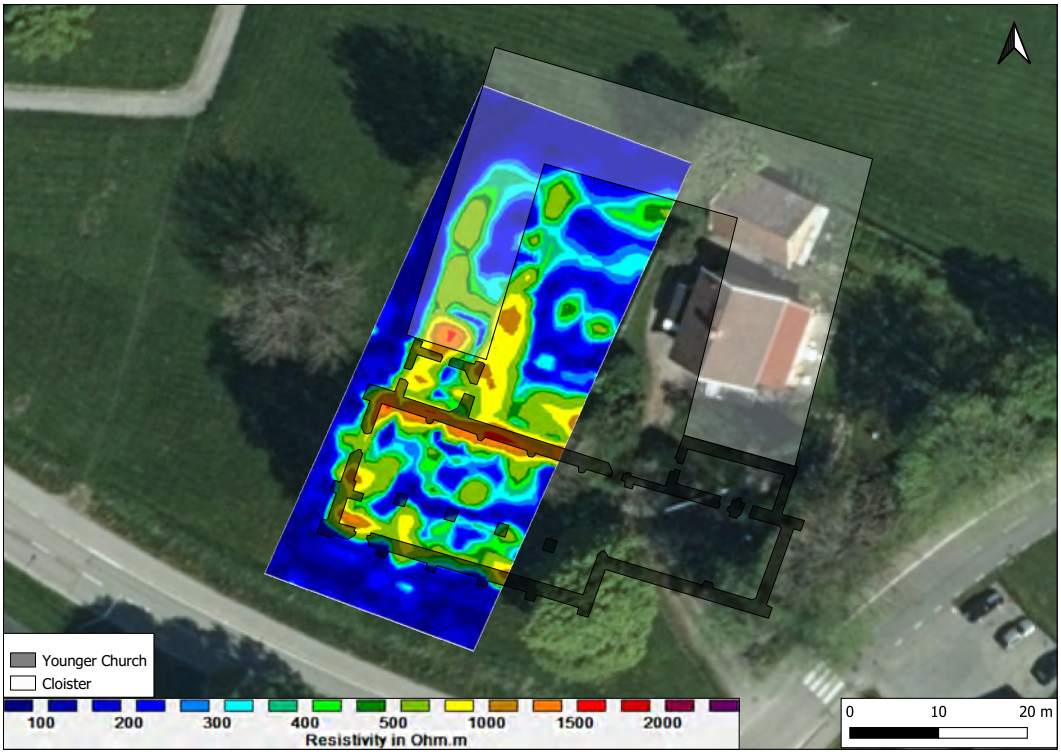

Figure 3.2: 3D Resistivity data of the Monastery Hill viewed from above. Electrode distance 1 meter. Depth slice from 1.08-1.74 meters. The younger church (black) and the cloister (white) is the extent of the Dominican monastery (af Ugglas, 1931; Ekre, 2007). Orthophoto © Lantmäteriet

Six depth slices of Wennerholm's data ranging from the surface down to 4.38 meters are presented in Figure 3.3 (Figure 1 in the Appendix for a larger image). The model shows a top view of the Monastery Hill survey area, with north being to the right. The six images show the variation of resistivity with depth, where the highest values are found closer to the surface. Deeper into the subsurface, the anomalies are starting to disappear. The scale bar is manually set to show the resistivity contrasts in a good and presentable way. The scale bar shows resistivity values ranging from below 100 Ω-m to above 2250 Ω-m (lowest value: 1.27 Ω-m; highest value: 2412.24 Ω-m). Elongated structures appears in the images. Some of the anomalies are striking in a N-S direction while some

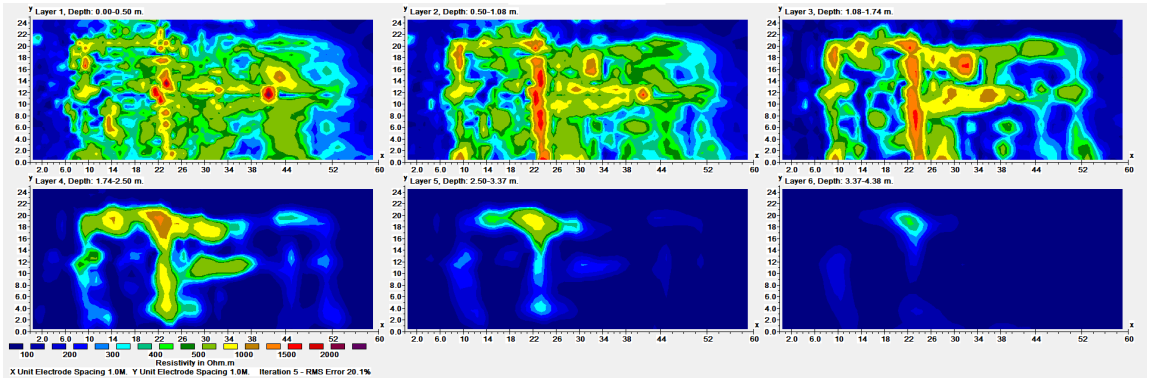

Figure 3.3: 3D Resistivity data of the Monastery Hill viewed from above. North is to the right in the image. Length 60 m; Width 25 m. Six different depth slices ranging from the surface (top left) to 4.38 meters (bottom right). Low resistivity values in blue to green colours, high resistivity values in yellow to red and purple. Electrode distance 1 meter. For a larger image, see Figure 1 in the Appendix.

are perpendicular to these in an E-W direction. As was seen in Figure 3.2, these areas of higher resistivity values can be interpreted as walls or foundations belonging to the Dominican monastery and the older church.

The first depth slice from the resistivity model using the data gathered in this study on the Monastery Hill is georeferenced together with the digitized Dominican monastery in Figure 3.4. Displayed on the map is also the old dam and the mill. The same colour scheme is used to be able to compare the results with Figure 3.2. It can be seen how the most northern cloister wall is aligned with the resistivity anomalies, but another elongated structure is appearing north of this, falling inside of the dam and the mill. Along the N-S striking cloister wall, other structures of high resistivity values are seen that were not visible in Figure 3.2. Instead of a dominant trend of N-S striking structures, the most structures seen are striking E-W.

The first depth slice together with the following slices from the data gathered in this study are presented in Figure 3.5 (Figure 2 in the Appendix). North is to the right in the image and the depth is ranging from the surface to 2.19 meters. The lowest resistivity value is 0.628 Ω-m and the highest value is 6714.6 Ω-m. Since the resolution is higher in this data (an electrode distance of 0.5 meter instead of 1 meter), more structures can be seen. This is also the reason for the interval between the depth slices being smaller. Many structures going in an E-W direction is visible. Structures going in a N-S direction can also be seen, forming squares together with the perpendicular structures.

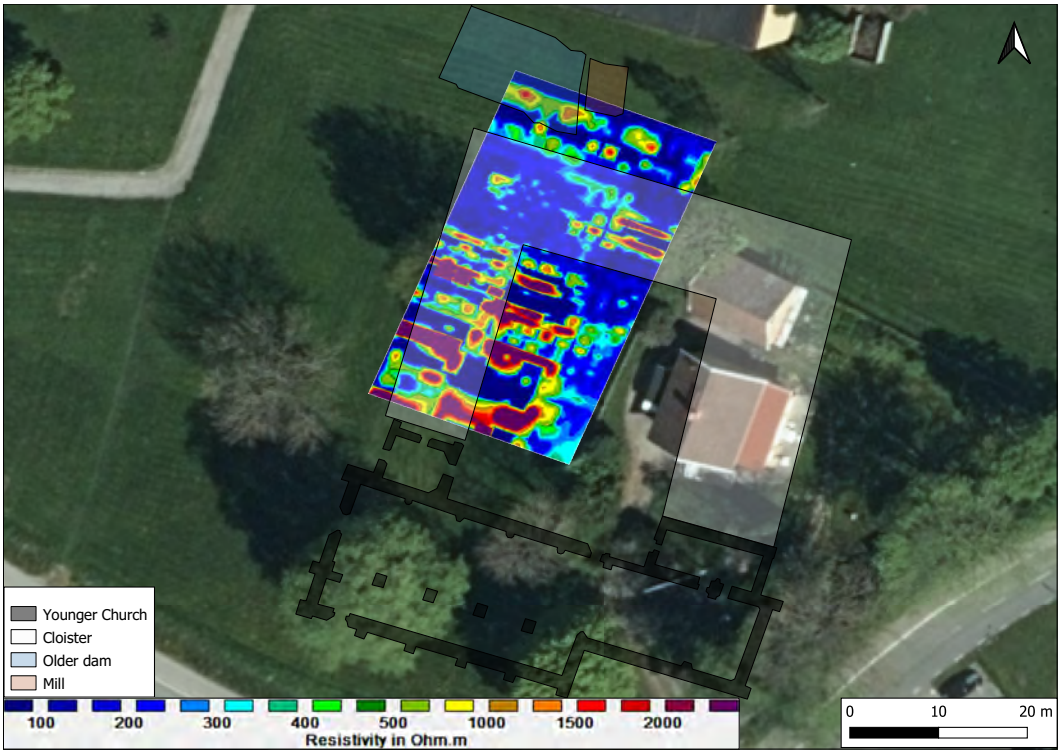

Figure 3.4: 3D Resistivity data of the Monastery Hill viewed from above. Electrode distance 0.5 meter. Depth slice from 0.0-0.25 meters. The younger church (black) and the cloister (white) is the extent of the Dominican monastery. The dam (blue) and the mill (brown) belonged to the older church (af Ugglas, 1931; Ekre, 2007).
Orthophoto © Lantmäteriet

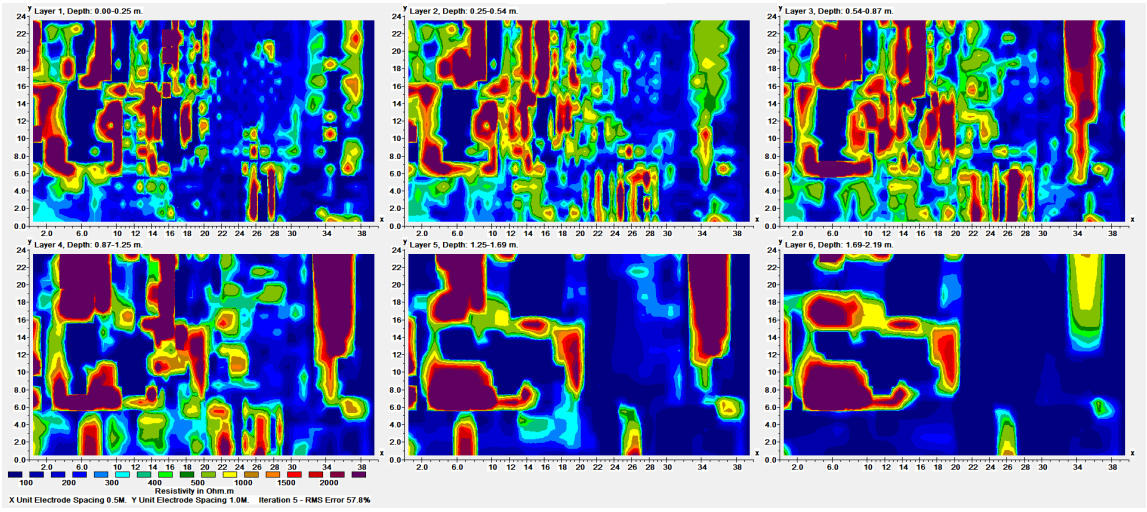

Figure 3.5: 3D Resistivity data of the Monastery Hill viewed from above. North is to the right in the image. Length 40 m; Width 24 m. Six different depth slices ranging from the surface (top left) to 2.19 meters (bottom right). Low resistivity values in blue to green colours, high resistivity values in yellow to red and purple. Electrode distance 0.5 meter. For a larger image, see Figure 2 in the Appendix.

The data from the resistivity survey done by Wennerholm was combined with the data gathered in this study resulting in a model covering all of the Monastery Hill west of the private property located on the hill. The result from Res3DInv is shown in Figure 3.6 (Figure 3 in the Appendix). It is presented in the same way as the other figures, with north being to the right and with the same colour scheme. The depth is ranging from the surface to 2.19 meters. The lowest resistivity value is 0.268 Ω-m and the highest is 5573.2 Ω-m. Close to the surface, thinner structures can be seen. Some is striking in an E-W direction and some N-S. Where they intersect they form squares. Deeper into the subsurface, larger structures appear, taking the shape of the monastery church as seen in the figures above.

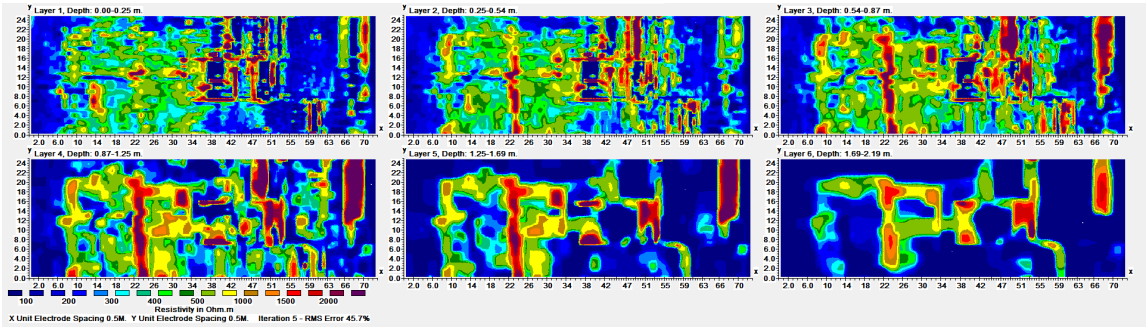

Figure 3.6: 3D Resistivity data of the Monastery Hill viewed from above. North is to the right in the image. Length 73 m; Width 25 m. Six different depth slices ranging from the surface (top left) to 2.19 meters (bottom right). Low resistivity values in blue to green colours, high resistivity values in yellow to red and purple. Combined electrode distance of 0.5 and 1 meter. For a larger image, see Figure 3 in the Appendix.

Before presenting these images georeferenced on a map, the Res3DInv results from the resistivity survey on the yard east of the house on the hill will be presented in Figure 3.7 (Figure 4 in the Appendix). North is to the right and the same colour scheme is used as for the other figures. The depth is ranging from the surface to 2.19 meters. The lowest resistivity value is 1.9 Ω-m and the highest value is 2055.8 Ω-m. Two structures can be seen in the six images. Farthest north is a clear elongated anomaly visible at all depths. At around 10 meters to the south, there is also an elongated structure appearing, best seen in the fourth slice at 0.87-1.25 meters depth. Between these two structures, there are other objects appearing of more diffuse shapes.

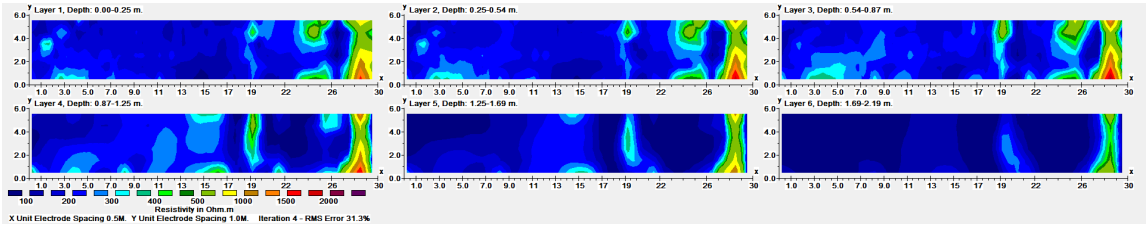

Figure 3.7: 3D Resistivity data of the Monastery Hill, east of the private property, viewed from above. North is to the right in the image. Length 30 m; Width 6 m. Six different depth slices ranging from the surface (top left) to 2.19 meters (bottom right). Low resistivity values in blue to green colours, high resistivity values in yellow to red and purple. Electrode distance of 0.5. For a larger image, see Figure 4 in the Appendix.

The different depth slices from Figure 3.6 and Figure 3.7 will now be presented georeferenced together with the churches and their surroundings in the following figures. Figure 3.8a to 3.9b will be shown together with the Dominican monastery. Figure 3.10a and 3.10b will be shown together with the older church. The old dam and the mill, the glassworks, the cable, and the wall located in the basement of the house are also included in all figures.

The surface layer (0.0-0.25 meter) of the resistivity surveys is shown in Figure 3.8a. Many anomalies seen as green colours are appearing in the southern half of the data covering the church, making it hard to do any interpretations. However, structures can still be seen that match the walls of the church. Except for the north-western part of the cloister, no structure of this can be seen in the resistivity. There are however other structures seen forming quadrangular objects. What is notable is how almost no high resistivity data can be seen in the E-W striking part of the cloister, except for two thin elongated structures. In the northernmost part of the survey done east of the house, can a structure be seen that is visible at all depth slices presented. There are three objects adjacent to this: the cloister, the glassworks, and the subsurface cable. The structures seen at a depth of 0.25-0.54 meter is not too different from the surface layer (Figure 3.8b). The walls of the younger church are more visible here and the structure following the most northern wall of the cloister is seen throughout the whole data (it is not a perfect match but it can be assumed that they belong to each other). The quadrangular objects are not as clear here but are still visible.

At a depth of 0.54-0.87 meter, the small structures merge into larger objects (Figure 3.9a). For example, what was two structures farthest north by the cloister wall and the dam, is now one large object. The northern wall of the younger church is now clearly visible. All walls of the younger church become more apparent at a depth of 0.87-1.25 meter (Figure 3.9b). Objects within the E-W striking part of the cloister are now appearing at this depth. A small elongated object can be seen at the center, east of the house. This structure is aligned with the wall located in the basement of the house.

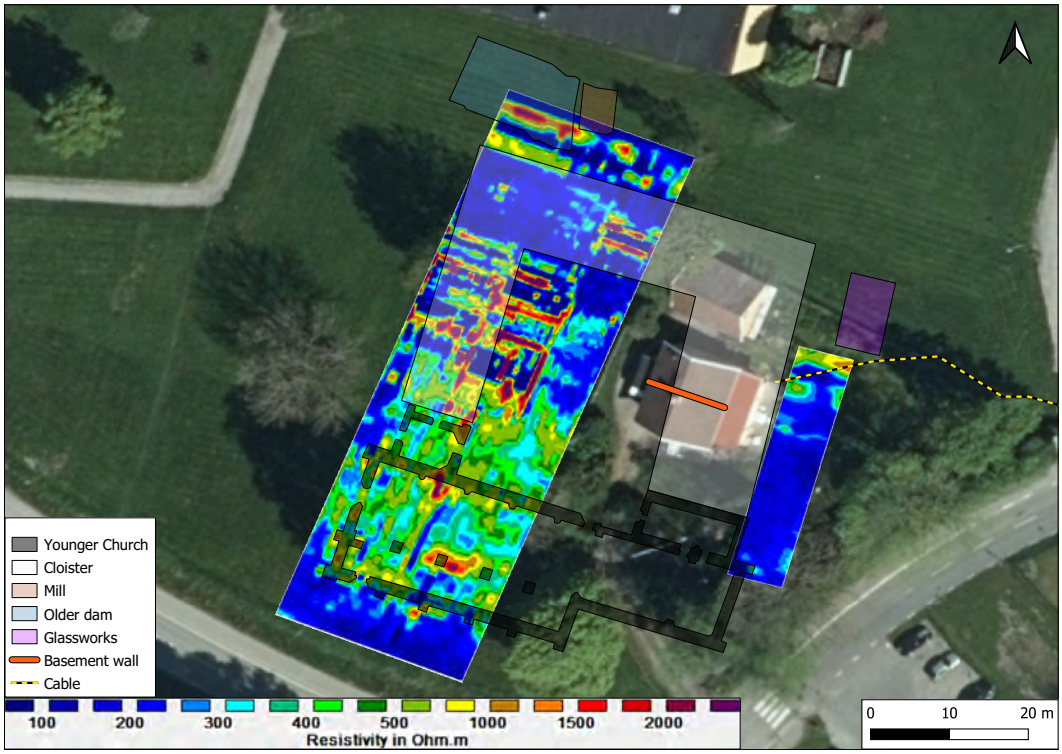

(a)

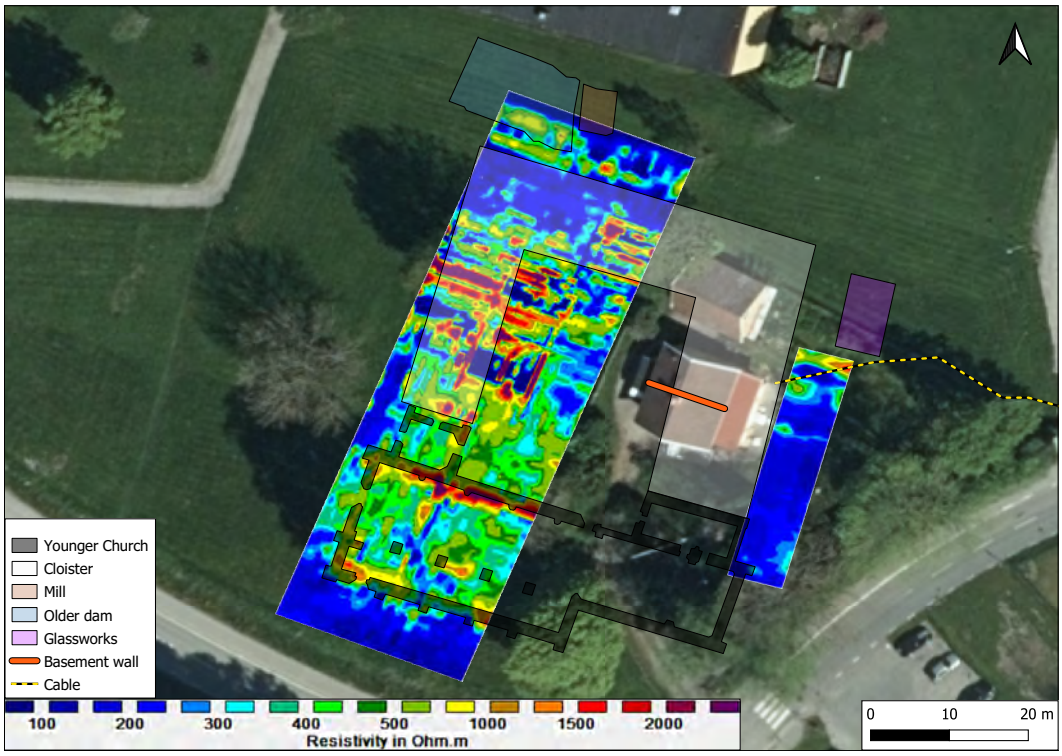

(b)

Figure 3.8: 3D Resistivity data of the Monastery Hill viewed from above. Depth slices from 0.0-0.25 meters (a) and 0.25-0.54 meters (b). The younger church (black) and the cloister (white) is the extent of the Dominican monastery. The dam (blue) and the mill (brown) belonged to the older church. The Dominican glassworks (purple), the subsurface cable (yellow dashed line), and the wall located in the basement (orange line) of the house are also placed on the map (af Ugglas, 1931; Ekre, 2007). Orthophoto © Lantmäteriet

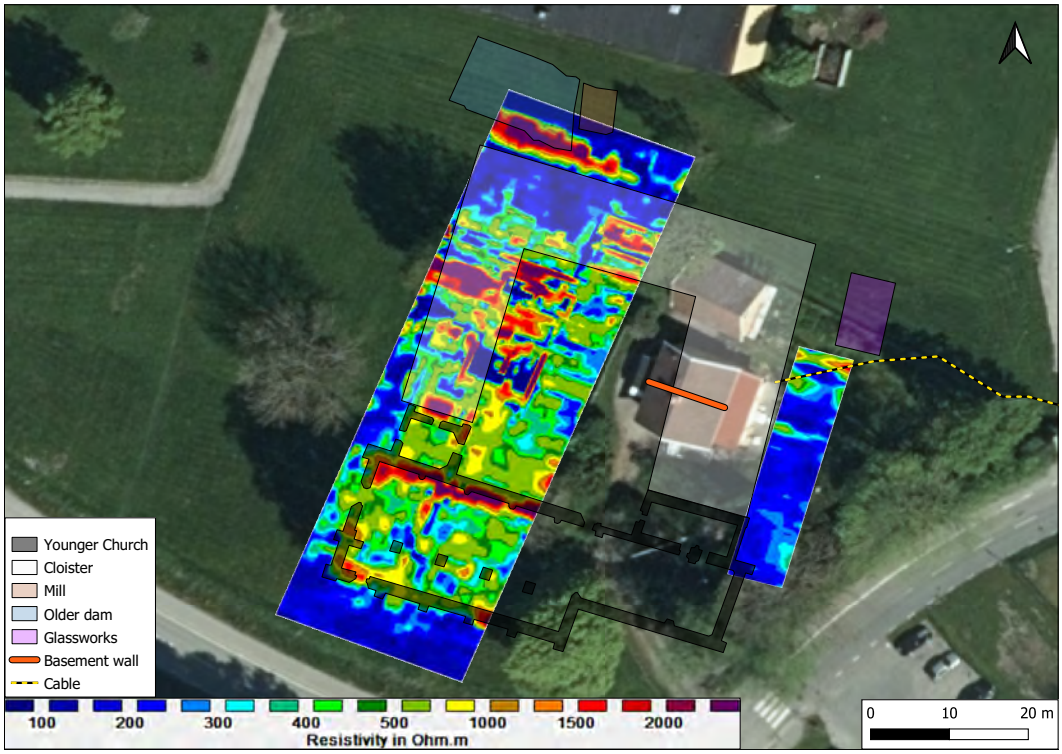

(a)

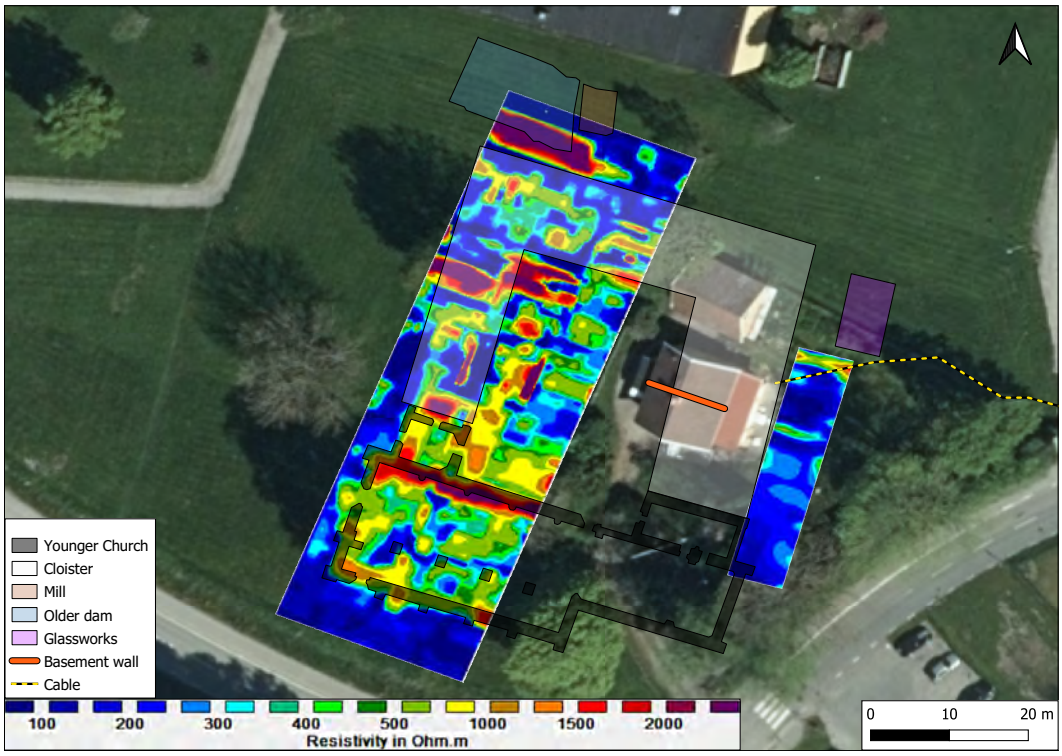

(b)

Figure 3.9: 3D Resistivity data of the Monastery Hill viewed from above. Depth slices from 0.54-0.87 meters (a) and 0.87-1.25 meters (b). The younger church (black) and the cloister (white) is the extent of the Dominican monastery. The dam (blue) and the mill (brown) belonged to the older church. The Dominican glassworks (purple), the subsurface cable (yellow dashed line), and the wall located in the basement (orange line) of the house are also placed on the map (af Ugglas, 1931; Ekre, 2007). Orthophoto © Lantmäteriet

Looking deeper into the subsurface, at a depth of 1.25-1.69 meter, the structures seen are comparable to the older church and the older dam and the mill (Figure 3.10a). The proposed buildings belonging to the Premonstratensian monastery (seen in Figure 1.8b) are excluded since the location of these is not known. It is therefore unnecessary to try to compare these with the resistivity data. The southern wall of the younger church can still be seen in the data, but the southern wall of the older church is now visible as well. The structures located inside of the the E-W striking part of the cloister that were seen in Figure 3.9b are no longer visible. No thin or small structures that have been seen in the middle of the survey area in the past figures are no longer visible either. Instead, quite rough structures are seen, almost in a step-like shape going upwards from the west to the east. The southern wall of the younger church is almost invisible at a depth of 1.69-2.09 meters, but fragments of the older church can still be seen (Figure 3.10b). The rest of the structures are not too different from Figure 3.10a.

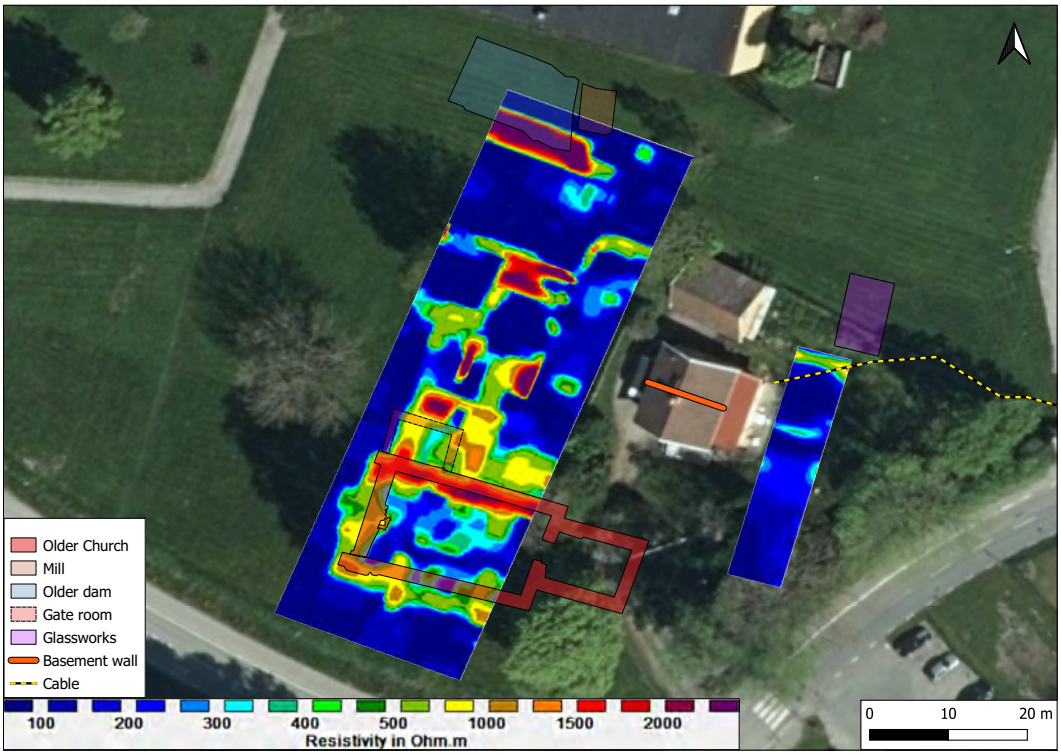

(a)

Figure 3.10: (a) 3D Resistivity data of the Monastery Hill viewed from above. Depth slice from 1.25-1.69 meters. The older church (red) with with the dam (blue) and the mill (brown). The Dominican glassworks (purple), the subsurface cable (yellow dashed line), and the wall located in the basement of the house (orange line) are also placed on the map (af Ugglas, 1931; Ekre, 2007). Orthophoto © Lantmäteriet

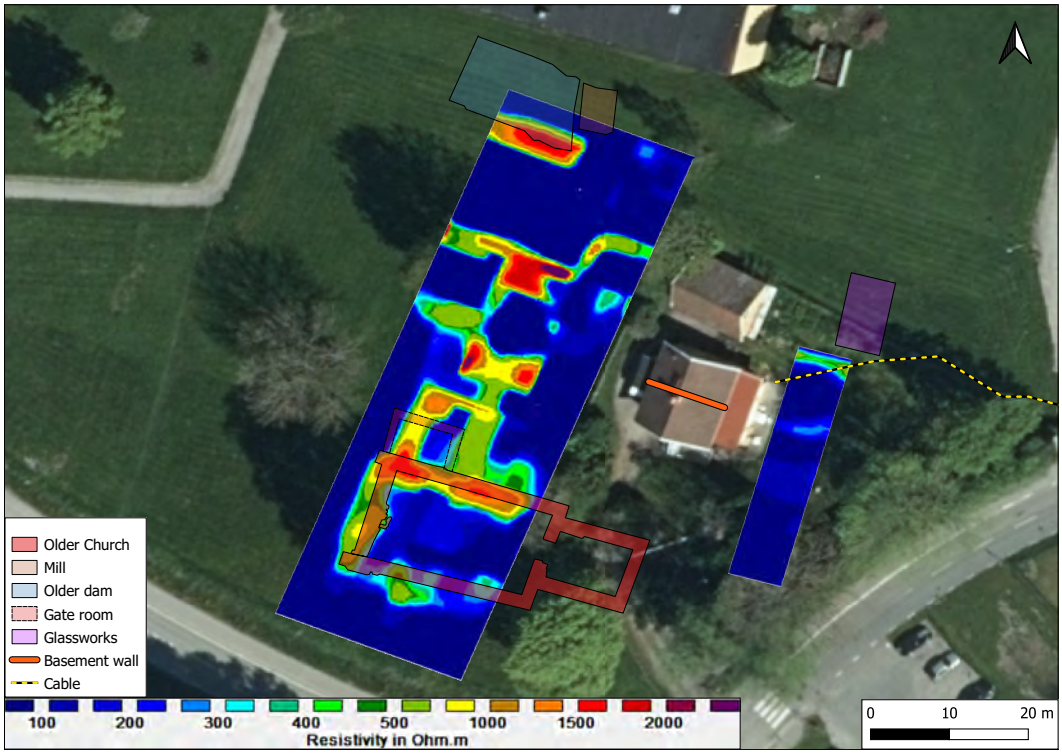

(b)

Figure 3.10: (b) 3D Resistivity data of the Monastery Hill viewed from above. Depth slice from 1.69-2.09 meters (b). The older church (red) with with the dam (blue) and the mill (brown). The Dominican glassworks (purple), the subsurface cable (yellow dashed line), and the wall located in the basement of the house (orange line) are also placed on the map (af Ugglas, 1931; Ekre, 2007). Orthophoto © Lantmäteriet

Even lower depth slices could have been presented, down to a level of 10.1 meters. These were not included since the structures of archaeological interest started to disappear below 2.19 meters. A full coverage displaying all depths is instead presented in the 3D models made in Voxler (Figure 3.11a and 3.11b). In these models it can be more difficult to differentiate the Dominican monastery from older objects underlying it. Instead, these 3D models can give a better understanding of how the archaeological features are placed in the soil and how they relate to each other. The same model is presented twice but viewed from different perspectives - looking towards north-west (Figure 3.11a) and looking towards north-east (Figure 3.11b). The figures show the same result as the models made in Res3DInv presented in the figures above. The difference is that instead of viewing depth slices, all of the data at all depths are viewed at the same time. The colour scheme is set from low resistivity values seen as blue to green, to high values seen as yellow to red, with a linear colour scale ranging between 0-1000 Ω-m. The low values have been made translucent to better see the structures. Why there is an object going vertically down to the bottom of the model at 10 meters depth where it flats out horizontally (Figure 3.11b) is either an error in the interpolation of the data or something of geological interest. This will be treated in the discussion section.

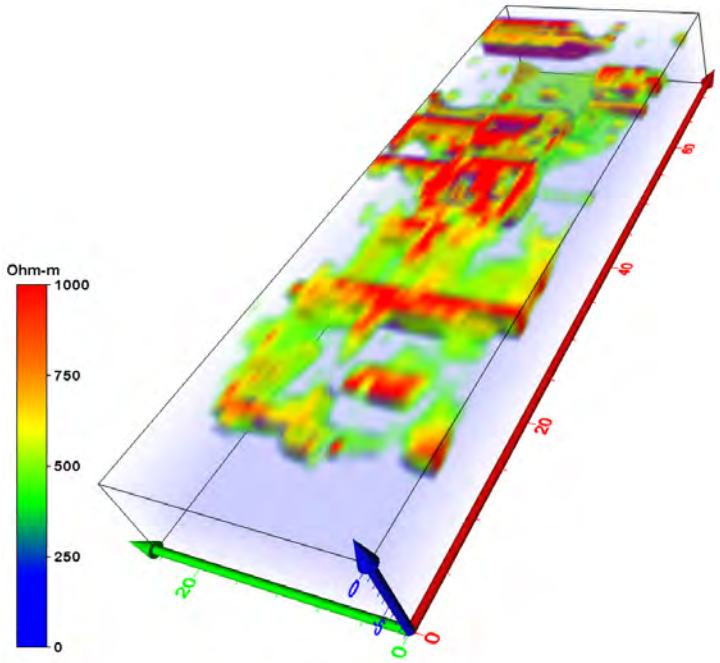

(a)

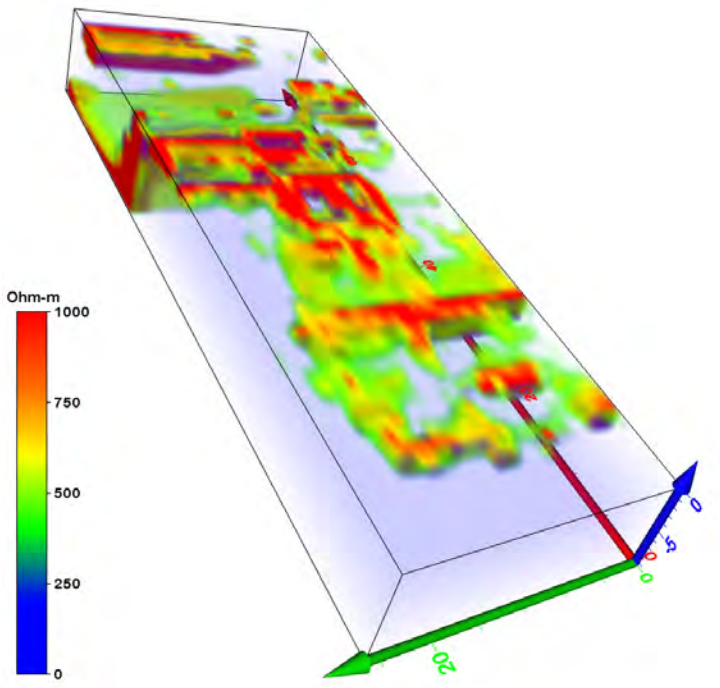

(b)

Figure 3.11: (b) 3D Resistivity model of the Monastery Hill looking towards north-west (a) and north-east (b). Length 73 m; Width 25 m; Depth 10 m. Linear colour scale from low resistivity in blue to high resistivity in red.

To illustrate the underlying geology on Monastery Hill, a 2D profile from the middle of the resistivity survey done east of the house is presented in Figure 3.12 (Figure 5 in the Appendix). This profile was chosen since this area does not contain as much archaeological remains that might interfere with the surrounding sediment. North is to the right in the figure. Note that a different colour scale is used for this figure (5-1000 Ω-m). The only areas with resistivity values less than 5 Ω-m are the corners in the bottom of the profile, which are artifacts that can occur in the interpolation of the model. With these excluded, there are no areas in the profile indicating that non-leached clay occurs (Figure 2.2). Most of the sediment has values above 25 Ω-m. The top two meters have values above 100 Ω-m. The quadrangular object seen around 19 meters along the profile is located by the wall seen in the basement of the house. It has a resistivity value of 700-800 Ω-m. The sediment below this feature should probably be of the same resistivity values as the areas to the left and right (10-50 Ω-m instead of 100-300 Ω-m), but an intermediate value has resulted from the interpolation process. Objects with values higher than 1000 Ω-m can be seen farthest to the right on the profile. These coincides with the elongated structure and the diffuse-shaped objects in the northern part of the survey (Figure 3.7).

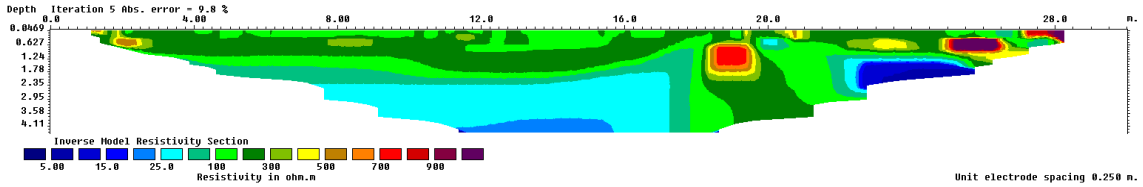

Figure 3.12: 2D Resistivity data of the Monastery Hill. Profile from the middle of the resistivity survey done east of the house. North to the right. Length 30 m; Depth 4.5 m. Low resistivity values in blue to green colours, high resistivity values in yellow to red and purple. Electrode distance 0.5 meter. For a larger image, see Figure 5 in the Appendix.

3.3 Magnetic Gradiometry

The interpolated results from the magnetic gradiometry survey are presented in Figure 3.13 together with the Dominican monastery. Here, the interesting anomalies can be seen in orange to red as negative values. What will be the focus in the discussion section is the E-W striking, large red structure in the northern part of the survey area. This feature will be called the ”E-W structure”. Other structures that can be seen are an elongated anomaly striking N-S in the eastern part of the survey area, along the fence belonging to the house; in the top left corner, anomalies appear aligned with the cloister wall; other anomalies are mainly seen as circular objects or other diffuse shapes.

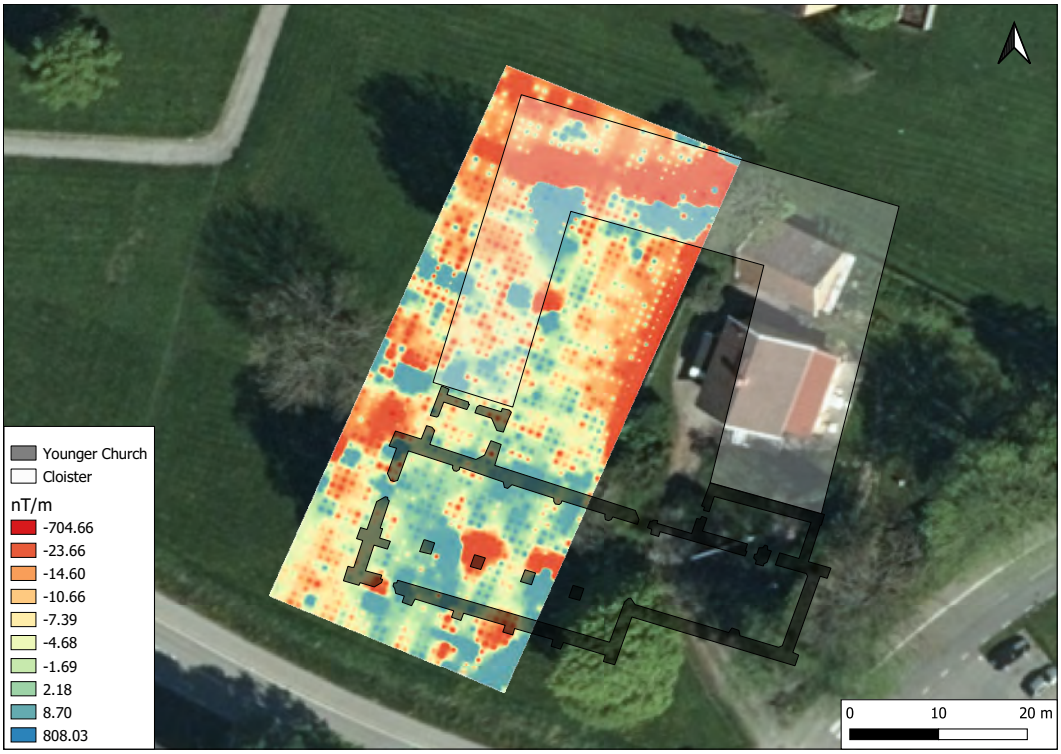

Figure 3.13: Interpolation of the gradiometry results (1 meter resolution) together with the Dominican monastery (af Ugglas, 1931; Ekre, 2007). Orthophoto © Lantmäteriet

Apart from the E-W structure, not much can be distinguished from the gradiometry data. However, when the data is compared to the GPR anomalies (first presented in Figure 3.1), more features can be interpreted. The polygonized anomalies from every 5 centimeter between 1.05-1.75 meters depth are seen together with the gradiometry data in Figure 3.14. Now it can be seen how the E-W structure is striking in the same direction as much of the GPR anomalies. Some of the otherwise diffuse gradiometry data can now be interpreted as well. For example, just below the E-W structure, there is an area of blue positive anomalies where GPR anomalies are absent. Below the blue area, GPR anomalies forming room-like squares are appearing in the same trend line as the E-W structure. Inside of these squares, negative gradiometry anomalies can be seen in orange to red colour. The southern side of the eastern square also seems to be aligned with the wall in the basement of the house. GPR anomalies forming a square are also seen in the top north-western part of the gradiometry survey area (Figure 3.14), falling inside of the strong negative gradiometry anomalies aligned with the cloister wall (Figure 3.13). Also, just north of the northern wall of the church (Figure 3.13), both GPR and negative gradiometry anomalies are seen striking in the same direction as the E-W structure (Figure 3.14).

A polygon was created of the E-W structure. This polygon can be seen together with the resistivity results from a depth of 0.25-0.54 meters in Figure 3.15. Now it can be seen that the E-W structure indirectly is visible in the resistivity data - the gradiometry anomaly is placed where the resistivity is low (with an exception for the area to the right). The older church is also placed in the figure to show how the E-W structure is striking in the same direction as the southern wall of the church.

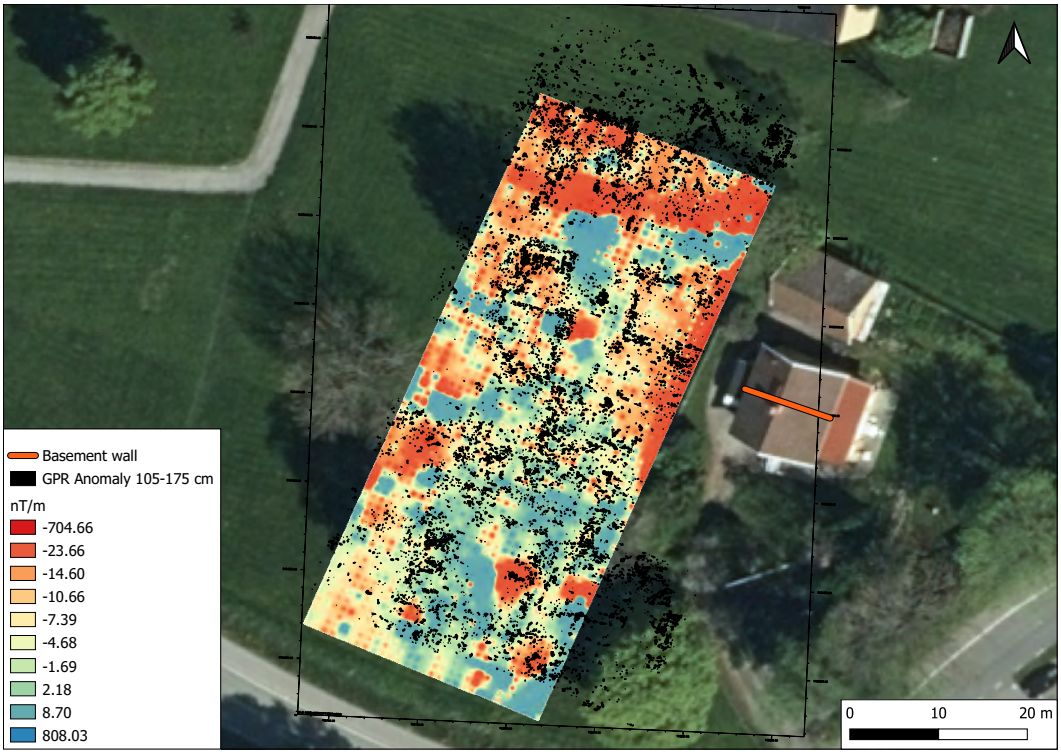

Figure 3.14: Interpolation of the gradiometry results (1 meter resolution) together with polygonized GPR anomalies. Orthophoto © Lantmäteriet

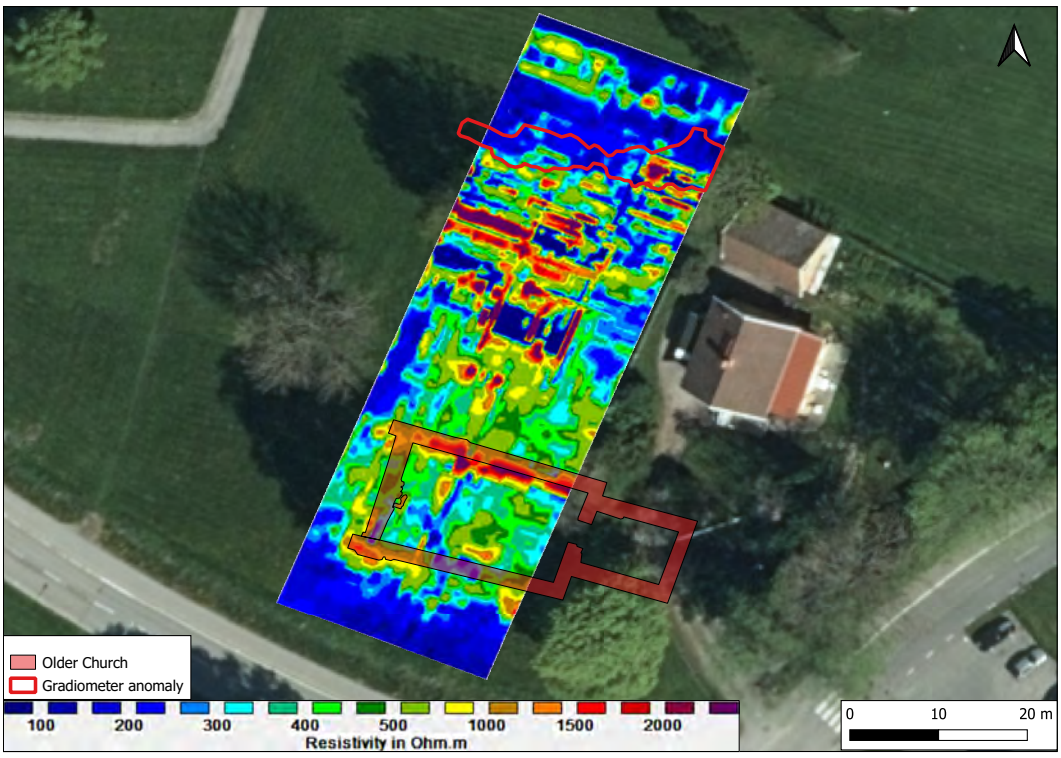

Figure 3.15: Highlighted anomaly from the gradiometer result on resistivity data of 0.25-0.54 meters depth. The older church is also placed on the map to compare its southern wall to the E-W structure (af Ugglas, 1931). Orthophoto © Lantmäteriet

4 DISCUSSION

4.1 Resistivity

4.1.1 Geology

From the 2D model of one of the resistivity profiles made (Figure 3.12), it can be interpreted that the post-glacial clay on Monastery Hill has been leached. However, if it means that a clay with a resistivity value above 25 Ω-m is a quick clay can not be concluded without further analyzes, such as sensitivity measurements. When looking on a resistivity profile made by Wennerholm (2021), it can be seen that the clay has been leached down to 11 meters depth. The leached clay is the reason the GPR measurements by Wennerholm (2021) worked as well as they did. As described in Chapter 2.1, the penetration depth of a GPR survey is highly dependent on the concentration of dissolved salts. The penetration depth in a non-leached clay would therefore be very shallow. The dissolution of the salts in the clay on Monastery Hill has favoured the GPR survey, allowing a deeper penetration than otherwise possible.

The quadrangular object at 19 meters along the resistivity profile from the smaller survey area (Figure 3.12) is aligned with the granitic stone wall located in the basement of the house. It can therefore be concluded that this object is that wall. What speaks against is the relatively low resistivity value of the object. It has a value of 700-800 Ω-m, whereas granite should have a value of 2000-1 000 000 Ω-m (Figure 2.2). The reason could be that the clay overlying the wall is lowering the resistivity of the granite in the interpolation.

What is noticeable in the model made in Voxler is the vertical structure of high resistivity extending downwards to the bottom of the model where it flats out horizontally (Figure 3.11b). Since there are no data points outside of the survey area, the model does not know how the subsurface looks like outside its boundaries. Therefore, the confidence of the interpolation is less along the borders. The vertical object of high resistivity could therefore just be an error in the interpolation. However, it should not be ignored how the horizontal feature only appears at the last few meters. If it is not an error, it could be that the resistivity survey is detecting bedrock. However, the bedrock surface is probably even further down, hence the relatively low resistivity values of around 500 Ω-m. What is seen could be a mixture of the resistivity between the clay and the bedrock. However, according to the model of the depth to bedrock (Figure 1.2b), the depth to bedrock should be 20-30 meters. This value does not need to be true though, since the map is an interpolation of point measurements from different observations in the surrounding area. There is no depth observation made within a radius of 100 meters from the survey area. While the model is produced with geologic common sense, it must

still be used with uncertainty. It is therefore possible that the depth to bedrock is shallower on the Monastery Hill than the depth model has interpolated it to be.

4.1.2 Archaeology

The resistivity surveys have proven to be a good tool to visualize what lies hidden under the surface on Monastery Hill. While the GPR data gives a clear image of the monastery, more structures can be seen from the resistivity, especially at depth. Some of the structures can be difficult to interpret, but others are aligned perfectly with the digitized maps of the churches. For example in Figure 3.2, it can be seen how the walls of the younger church are clearly visible in the resistivity model. Especially the northern wall is seen as higher resistivity values. This wall is very robust according to af Ugglas (1931, p. 246) which probably is the explanation for this. What can not be seen as clearly in the model however, is the gate room by the left side of the northern wall of the church and the outer wall of the cloister going northward until it takes a turn to the east. Even though it is not the exact same image, there are two structures in the resistivity model (Figure 3.2) that go northward until they take a turn to the east. The resistivity might not view the same structures as the GPR, but similarities can be seen. It might be that the cloister walls can not be seen in the resistivity data, but the floor within the walls, or the ground outside of the walls, is what becomes visible.

In Figure 3.8a, structures that look like walls of different rooms can be seen. For a better visualization, a zoomed in version of this figure is presented in Figure 4.1. Here, a square is seen to the left, which looks like a room. It has a surface area of 75 m^2. A similar feature is placed by the lower right corner of this room, with a surface area of 60 m^2. North of the lower room is an elongated feature that looks like a wall. This may then be two rooms and a structure that can be interpreted as a hallway. The hallway has a surface area of 30 m^2. Similar rooms can be seen in the radar images at lower depths (Figure 3.1), but a perfect match between the resistivity and the GPR anomalies has not been acquired. This means either that the structures seen in the resistivity are other objects, or that some sources of error have displaced the structures. The resistivity models assume that the profiles have been made in completely straight lines. Even though this is the goal when gathering the data, it might not be reality. This can explain why some of the structures are not aligned with the GPR data or the digitized monastery. A better method to insure perfectly straight lines would have been to create a grid before starting the measurements. Also, a better GPS, like the Leica RTK used for the GPR measurements, would be preferable instead of a hand-held GPS. However, since the walls of the churches are matching well with the resistivity data, it can be safe to conclude that the models are correct and have been georeferenced properly. Assuming this, it can be concluded that the resistivity models show rooms built on top of the rooms seen in the radar images. The rooms from the resistivity models are at a much shallower depth than the rooms from the radar images (the first half meter instead of around 1.5 meters down). They are also parallel to the walls of the younger church and not in an oblique angle as the rooms in the radar images are. They would therefore belong to the Dominican monastery built on top of older rooms, perhaps belong to a Premonstratensian monastery. If the whole survey area had been done with an electrode distance of 0.5 meters, maybe more room-like structures would have appeared.

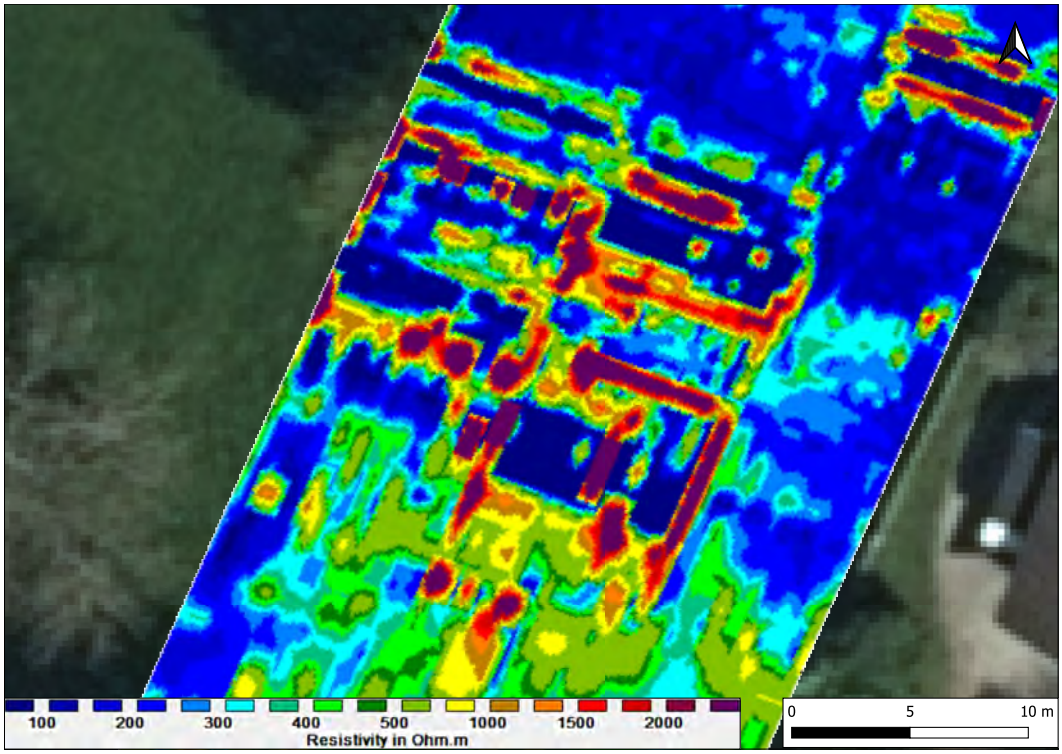

Figure 4.1: 3D Resistivity data of the Monastery Hill viewed from above, zoomed in over the area of the rooms. Depth slice from 0.0-0.25 meters. Orthophoto © Lantmäteriet

The walls of the rooms seen in Figure 4.1 have a resistivity above 2000 Ω-m. It it not known if these rooms were built in both stone and brick, like much of the younger church, or only in brick. However, since these walls are thinner than the walls of the church, it can be assumed that at least the majority of the walls were made of brick. As described in the method (Chapter 2.2), the resistivity of a brick wall can vary a lot depending on building technique and fractures. Because the buried walls are 500 years old, it can be assumed that the walls are quite damaged. This can explain the high resistivity, especially if there are air-filled cavities in the walls. Air-filled cavities can also explain the relative high resistivity values around all objects of high resistivity, if air is trapped between the archaeological features and the soil.

In the northernmost part of the survey area, two structures can be seen in Figure 3.8a and 3.8b. The southern structure is aligned with the cloister wall and is thus interpreted to be this wall. The northern structure is interpreted to belong to the dam and the mill that was used by the older church. At lower depths (Figure 3.9a to 3.10b), these two objects are merged together. The reason is probably that the resolution of the data decreases with depth.

What the different structures seen in the survey from the east of the house are is more difficult to say since the area is small and outside of the archaeological maps. What can be said is that the structure seen in the middle of the model probably is the stone wall located in the basement of the house (Figure 3.9b). It is tempting to interpret the northern structure seen at all depths (Figure 3.8a to 3.10b) to be the glassworks. Ekre's (2007) placement of the glassworks is just approximate, so the glassworks could therefore be located farther to the south-west, aligning with the resistivity data. If the structure is not the glassworks, it is probably an extension of the cloister. It is not likely that it is

the cable, since the cable should be located diagonal to the structure. It does not seem that the cable is appearing at all in the resistivity model.

Just north of the northern wall of the younger (and older) church is an area of high resistivity (for example Figure 3.9b). This area was not excavated by af Ugglas (1931), but he had an idea of what it might be. Buttresses were found on the outer sides of the walls of the younger church. These are however missing from the northern wall (compare the outside of the northern wall to the rest of the walls in Figure 1.8a). It is therefore believed that an other building belonging to the monastery was placed by the northern wall that acted as support (af Ugglas, 1931, p. 246). This building is likely what is seen in the resistivity data. Considering that af Ugglas (1931) made the connection that a building must have been located by the northern wall of the younger church, it is surprising that Ekre (2007, p. 146) did not include this in his drawing of the Dominican monastery. This building is therefore added to be a part of the cloister (Figure 4.2). How it continues to the right of the opening in the northern wall and how it connects to the eastern cloister is left to be said.

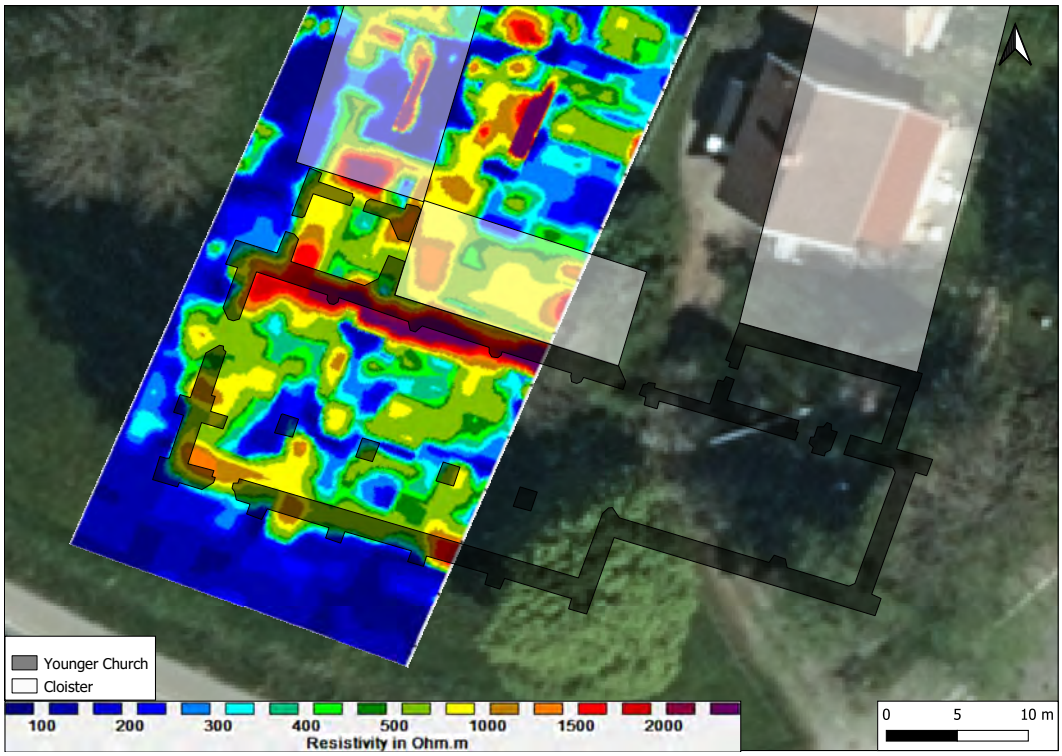

Figure 4.2: Building added to the cloister, as proposed by af Ugglas (1931). Orthophoto © Lantmäteriet

4.2 Magnetic Gradiometry

The magnetic gradiometry shows both interesting structures as well as features that can be ignored. Rocks have been placed on the surface by archaeologists to visualise the extent of the Dominican monastery. These can be seen as somewhat circular red spots in the southern part of the survey area (Figure 3.13). The N-S striking red border in the eastern part of the image close to the house is probably the fence belonging to the property. With these areas excluded, no clear result of a

monastery can be seen, except for the structure appearing in an E-W direction in the northern part. It is interesting how the churches can not be seen from the gradiometry survey while the E-W structure unmistakably appears. It can be hard to determine what this structure is without an excavation but two ideas will be discussed that might give an explanation to this anomaly.

The first idea is if this is a wall built in a different material than the rest of the remnants on the Monastery Hill that is favourable for the instrument used. If the brick walls of the Dominican monastery do not appear in the survey, maybe a stone wall would appear instead. A non-magnetic stone wall of granite would appear as a negative anomaly. Simultaneously, this structure can indirectly be seen in the resistivity model as an area of low resistivity (Figure 3.15). This contradicts the idea of the structure to be a stone wall, since this would give high resistivity values. This structure must be of a low-resistivity material that gives a high negative magnetic anomaly. This leads to the second idea that the structure is an old ditch. As described in Chapter 2.3, a ditch can acquire a negative anomaly if it is leached from magnetic minerals. Since the structure is placed by the side of the hill, it is plausible that groundwater and precipitation are flowing from the top of the hill and downward. In fact, the ground downslope north of the hill is very wet with a peaty topsoil, supporting this claim.

No depth information can be gathered from the magnetic gradiometry. It can however be concluded that the E-W structure should be placed either above 0.87 meters depth or below 1.25 meter, since there is another structure of higher resistivity appearing at this interval (Figure 3.9b). As can be seen in Figure 3.15, the area of low resistivity shares the same general direction as the gradiometry anomaly, favouring the idea of the structure being placed above 0.87 meters depth. What is favouring the idea of the structure being placed below 1.25 meters depth is that it seems to be parallel to much of the anomalies seen from the GPR data at 1.05-1.75 meters depth (Figure 3.14 and 3.15).

4.3 Future Excavations

From the results and interpretations of the Monastery Hill, a proposal is given for future archaeological excavations. While it may be of interest to yet again excavate the two churches to do further studies with the archaeological knowledge of today, it would be intriguing to continue where af Ugglas (1931) ended. One proposed excavation area is therefore by the beginning of the western cloister, covering the rooms found by the resistivity survey (lower excavation area in Figure 4.3). The proposed excavation has a surface area of $370\,m^2$. The rooms are located very shallow and should be found in the top half meter. A second excavation is proposed to cover the structure found by the magnetic gradiometry survey (upper excavation area in Figure 4.3). It can only be speculated if this structure is a wall, a ditch, or something completely different. Only an excavation will give truth to what it is. The excavation area has a surface area of $330\,m^2$. It was previously discussed in Chapter 4.2 if this structure is located above 0.87 meters or below 1.25 meters depth. The depth of the excavation is therefore dependent on where it will be found. Otherwise, the structure seen in the resistivity data in between this interval (Figure 3.9b) will also be found.

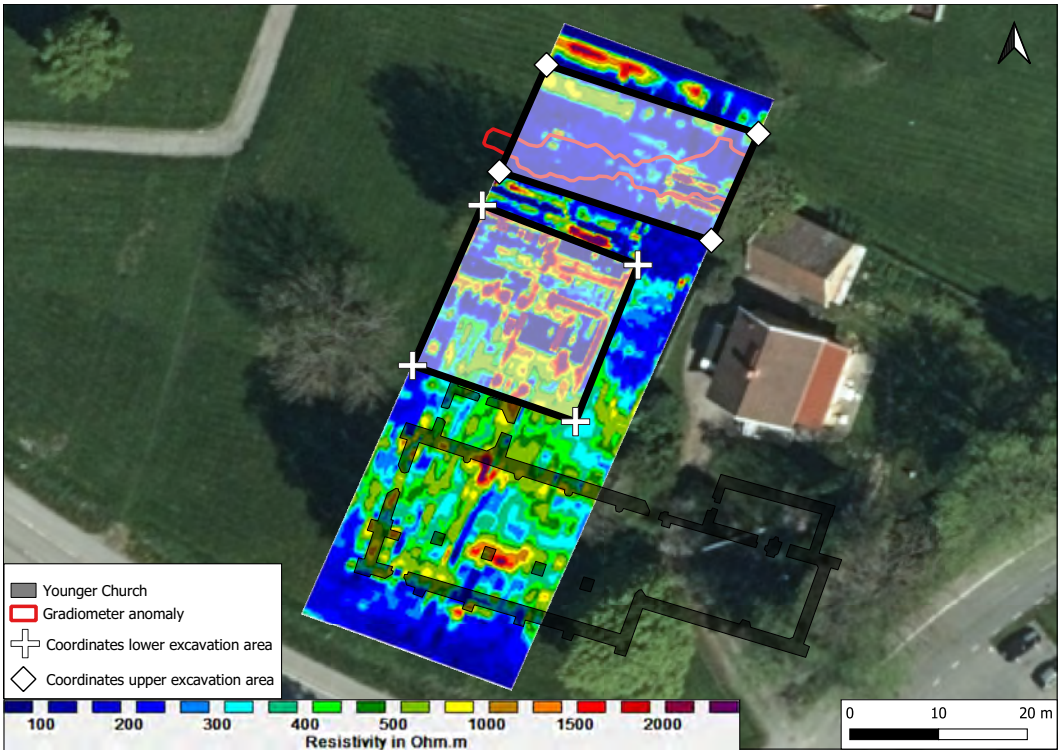

Figure 4.3: 3D Resistivity data of the Monastery Hill viewed from above. Depth slice from 0.0-0.25 meters. Two proposed excavation areas are placed on the map, one upper and one lower. Coordinates in Table 4.1. The younger church (af Ugglas, 1931) and the gradiometry anomalies are also added to the map. Orthophoto © Lantmäteriet

The coordinates of the corners for the lower and the upper excavation areas marked in Figure 4.3 as white crosses and white diamonds respectively are noted in Table 4.1 (in SWEREF99 TM).

Table 4.1: Lower and upper excavation area coordinates (SWEREF99 TM), marked as white crosses and white diamonds respectively in Figure 4.3.

Lower excavation	X	Y
NW	332061.392	6435960.802
NE	332078.943	6435954.067
SW	332053.535	6435942.741
SE	332071.903	6435936.414
Upper excavation	X	Y
NW	332068.637	6435976.618
NE	332092.515	6435968.863
SW	332063.331	6435964.578
SE	332087.209	6435956.822

5 CONCLUSIONS

The GPR data gives a clear representation of the Dominican monastery, but additional features can be seen from the resistivity images, especially at depth. The signal attenuation in clay is generally high, leading to shallow penetration depths for GPR surveys. However, the resistivity survey has shown that the clay on the Monastery Hill has been leached, with resistivity values above 100 Ω-m in the top two meters of the soil. This leads to a deeper penetration depth for the GPR survey than otherwise possible.

Even though more features can be seen from the resistivity (e.g., the room-like features and the building located just north of the northern wall of the younger church), it can be harder to interpret the resistivity data than the GPR data for the inexperienced. Therefore, it is great that the resistivity survey has been conducted in this study area where excavation maps of the churches are available and a GPR survey already had been made. This gives a better understanding of the data and this study can be used as reference material for future resistivity surveys and for planning potential excavations in the survey area. From this study it is suggested that joint GPR and resistivity surveys should be used whenever justified geologically and financially.

The room-like features seen in the resistivity data are shallower than the rooms seen in the GPR-data, and they are not aligned with each other. The rooms from the GPR must therefore be of older age. This may be evidence for a Premonstratensian monastery to have existed before the Dominican monastery.

The instrument used for the magnetic gradiometry survey did not do well for visualizing the Dominican monastery or the older church. Instead, it found a structure (called the the E-W structure in previous chapters) not discovered by the resistivity nor the GPR. The E-W structure is an object displaying a negative magnetic anomaly and is of a low resistivity material. It has been interpreted to be a ditch since a leached ditch will have these features. However, this will not be certain without an archaeological excavation.

To improve the gradiometry results, a more advanced gradiometer that can do surveys continuously would be useful. This would obviously be much faster than recording three measurement points at every meter as done in this study. Doing continuous measurements would complement the GPR survey well.

It is possible that the depth to bedrock is shallower than 20-30 meters on the Monastery Hill, as the model of the depth to bedrock otherwise implies. Higher resistivity values close to 10 meters depth might indicate that the survey is detecting bedrock. Clay has the ability to apparently lower the resistivity value of underlying material. This is probably what is happening at 10 meters depth, and also for the stone wall seen in the survey east of the house on the Monastery Hill.

Geophysical methods have been proven very useful in describing the archaeology and the near-surface geology on the Monastery Hill and it shows big potential for use elsewhere. Including the survey done by Wennerholm (2021), three methods have been mutually compared (GPR, resistivity and magnetic gradiometry). It has been shown how they all have their specific pros and cons and illuminate different archaeological features in the subsurface.

REFERENCES

af Ugglas, C. R. (1931). *Lödöse (Gamla Lödöse) - Historia och Arkeologi*. Elanders Boktryckeri.

Andersson, F., & Möhl, T. (2021). *Geophysical Methods for Describing Archaeology and Near-Surface Geology at Lödösehus, Lödöse, SW Sweden* (Master's thesis). Göteborgs Universitet.

Åström, S., Eklund, D., & Lindahl, S. (2011). Hydrodynamisk modell för Göta älv - Underlag för analys av vattennivåer, strömhastigheter och bottenskjuvspänningar. *SGI - Göta älvutredningen, delrapport 3*.

Carlsson, K. (1995). Lödöse - En medeltida storstad. In A. Boqvist (Ed.), *Skara i medeltid - Staden Stiftet Landskapet* (pp. 152–159). Rydins Tryckeri AB.

Conyers, L. B. (2018). *Ground-penetrating Radar and Magnetometry for Buried Landscape Analysis*. Springer.

Council of Europe. (1992). European Convention on the Protection of the Archaeological Heritage (Revised). *Valetta, 16.I.*

De Donno, G., Di Giambattista, L., & Orlando, L. (2017). High-resolution investigation of masonry sampler through GPR and electrical resistivity tomography. *Construction and Building Materials*, *154*, 1234–1249.

Doolittle, J. A., & Collins, M. E. (1995). Use of soil information to determine application of ground penetrating radar. *Journal of Applied Geophysics*, *33*, 101–108.

Ekre, R. (1968). *Ny Bild av Medeltidens Lödöse*. Förenade Tryckerier.

Ekre, R. (1991a). Borg och kungsgård i Lödöse. In C. Aarsrud, P. Nissen, K. R. Svensson, K. Rosell, & C. Winberg (Eds.), *Skärvor och fragment - Kring medeltid i Älvsborgs län* (pp. 54–72). Risbergs Tryckeri AB.

Ekre, R. (1991b). Om den medeltida myntningen i Lödöse. In C. Aarsrud, P. Nissen, K. R. Svensson, K. Rosell, & C. Winberg (Eds.), *Skärvor och fragment - Kring medeltid i Älvsborgs län* (pp. 32–48). Risbergs Tryckeri AB.

Ekre, R. (2007). Kloster i Lödöse. In J. Hagberg (Ed.), *Kloster och klosterliv i det medeltida Skara stift* (pp. 109–158). Solveigs Tryckeri.

Ekre, R., Hylander, C., & Sundberg, R. (1994). *Lödösefynd - ting från en medeltidsstad*. Bohusläningens Boktryckeri AB.

Fassbinder, J. W. (2015). Seeing beneath the farmland, steppe and desert soil:

magnetic prospecting and soil magnetism. *Journal of Archaeological Science*, *56*, 85–95.

Fredén, C. (1986). *Beskrivning till jordartskartan, Göteborg NO (Serie Ae, Nr 40)*. Sveriges Geologiska Undersökning.

Karlsson, P., Westergaard, B., Stenqvist, L., & Trinks, I. (2014). Georadarundersökning på Kjesarterrassen, Gunnebo slott, Mölndal. *Swedish National Heritage Board*.

Klingberg, F., Påsse, T., & Levander, J. (2006). Bottenförhållanden och geologisk utveckling i Göta älv. *Sveriges Geologiska Undersökning*.

Milsom, J., & Eriksen, A. (2011). *Field Geophysics*. John Wiley & Sons, Ltd.

Musset, A. E., & Khan, M. A. (2000). *Looking into the Earth - An Introduction to Geological Geophysics*. Cambridge University Press.

Order of Prémontré. (2021). *Who we are*. https://premontre.org/about-us/who-we-are/

Ordo Praedicatorum. (2021). *History*. https://www.op.org/history/

Rundkvist, M., & Viberg, A. (2014). Geophysical Investigations on the Viking Period Platform Mound at Aska in Hagebyhöga Parish, Sweden. *Archaeological Prospection*.

Sällfors, G. (2013). *Geoteknik: jordmateriallära, jordmekanik*. Cremona.

SGI. (2012). Skredrisker i Göta älvdalen i ett förändrat klimat: Slutrapport Del 3 - Kartor. *SGI - Göta älvutredningen*.

SGI. (2018). Metodik för kartläggning av kvicklera, Vägledning. *SGI publikation*, *46*.

SGI. (2020, December 11). *Jordarter*. https://www.sgi.se/sv/kunskapscentrum/om-geoteknik-och-miljogeoteknik/geoteknik-och-markmiljo/jordmateriallara/lera-och-kvicklera/

SGU. (2021, May 10). *SGUs Kartvisare*. https://apps.sgu.se/kartvisare/kartvisare-skred.html

Stevens, R. L., Rosenbaum, M. S., & Hellgren, L. G. (1991). Origin and engineering hazards of Swedish glaciomarine and marine clays. *Quaternary Engineering Geology*, *7*, 257–264.

Storm, K. (2021, April 23). *Vår historia*. https://www.svenskakyrkan.se/sigtuna/var-historia

Triumf, C. A. (1992). *Geofysik för geotekniker*. Byggforskningsrådet, T31, Stockholm.

Viberg, A., Trinks, I., & Lidén, K. (2011). A Review of the Use of Geophysical Archaeological Prospection in Sweden. *Archaeological Prospection*, *18*, 43–56.

Viberg, A., & Wikström, A. (2014). St. Mary's Dominican Convent in Sigtuna Revisited. *Fornvännen*, *106*.

Wennerholm, E. (2021). *Unpublished manuscript* (Master's thesis). Göteborgs Universitet.

Westergaard, B., Eriksen, K., & Trinks, I. (2019). Drottningholms slott, Stockholm: Georadarundersökning. *Arkeologerna*.

Widéen, H. (1944). Klosterkyrkorna i Lödöse. *Fornvännen*, 311–321.

Appendix

List of figures of the resistivity models:

- Figure 1: Resistivity model of the data gathered by Wennerholm (unpublished). (Same as Figure 3.3.)
- Figure 2: Resistivity model of the data gathered in this study on the Monastery Hill. (Same as Figure 3.5.)
- Figure 3: Resistivity model of the data gathered in this study combined with the data from Wennerholm (unpublished) on the Monastery Hill. (Same as Figure 3.6.)
- Figure 4: Resistivity model of the data gathered on the yard east of the house on the hill. (Same as Figure 3.7.)
- Figure 5: 2D resistivity model of the middle profile from the yard east of the house on the hill. (Same as Figure 3.12.)

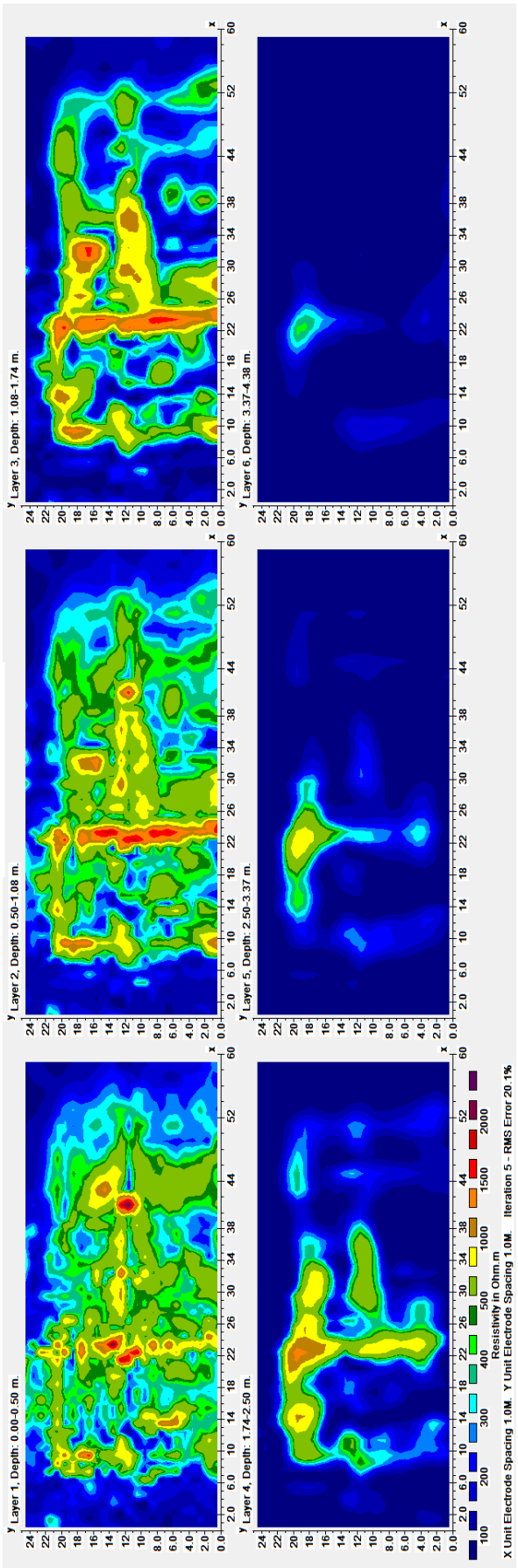

Figure 1: 3D Resistivity data of the Monastery Hill viewed from above. North is to the right in the image. Length 60 m; Width 25 m. Six different depth slices ranging from the surface (top left) to 4.38 meters (bottom right). Low resistivity values in blue to green colours, high resistivity values in yellow to red and purple. Electrode distance 1 meter..

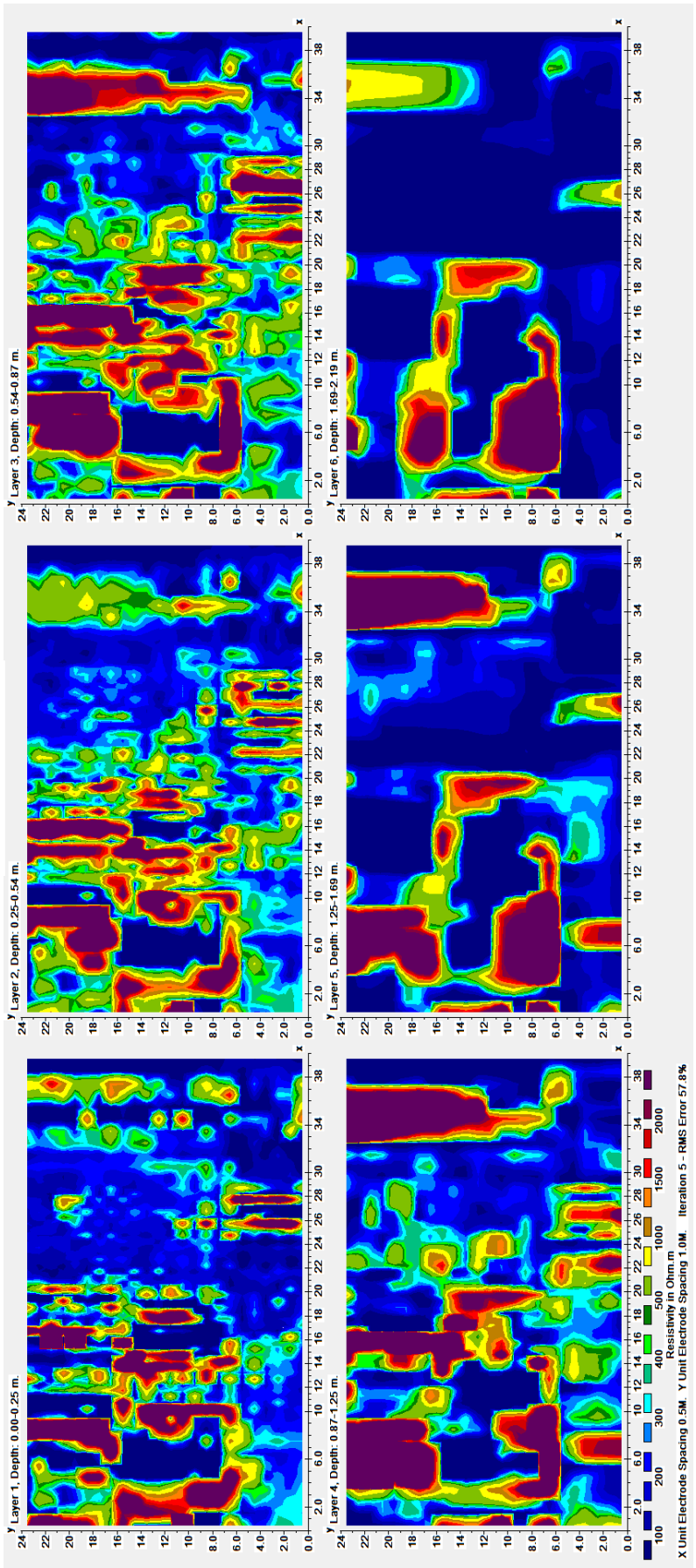

Figure 2: 3D Resistivity data of the Monastery Hill viewed from above. North is to the right in the image. Length 40 m; Width 24 m. Six different depth slices ranging from the surface (top left) to 2.19 meters (bottom right). Low resistivity values in blue to green colours, high resistivity values in yellow to red and purple. Electrode distance 0.5 meter

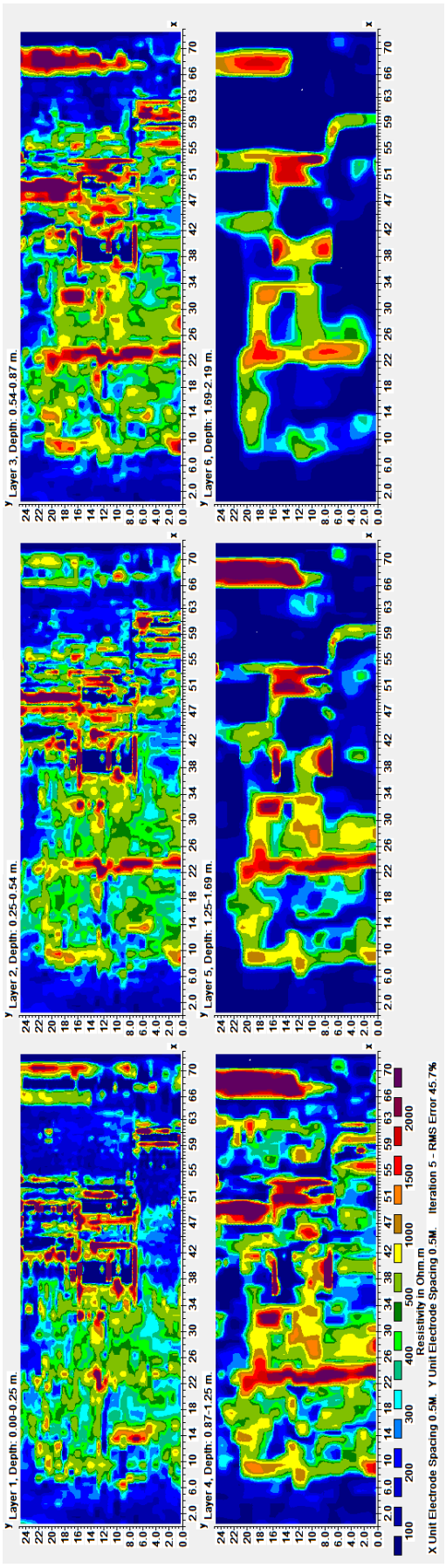

Figure 3: 3D Resistivity data of the Monastery Hill viewed from above. North is to the right in the image. Length 73 m; Width 25 m. Six different depth slices ranging from the surface (top left) to 2.19 meters (bottom right). Low resistivity values in blue to green colours, high resistivity values in yellow to red and purple. Combined electrode distance of 0.5 and 1 meter.

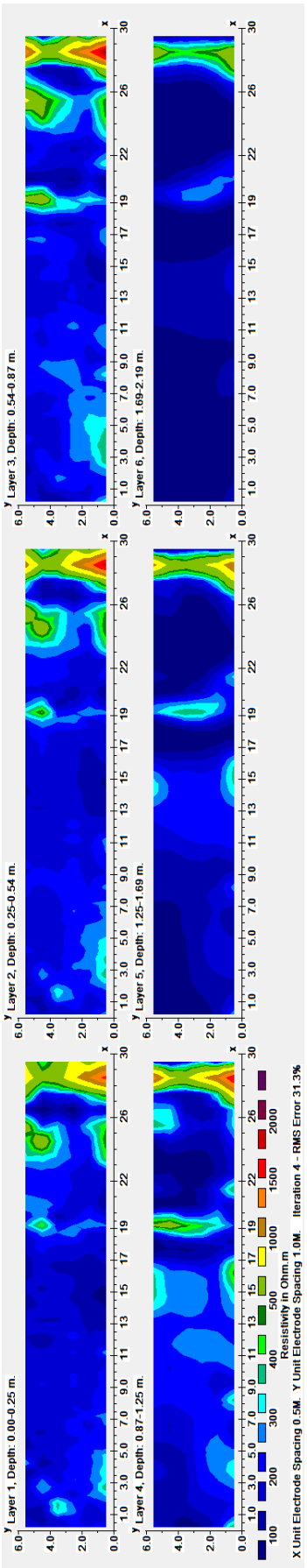

Figure 4: 3D Resistivity data of the Monastery Hill, east of the private property, viewed from above. North is to the right in the image. Length 30 m; Width 6 m. Six different depth slices ranging from the surface (top left) to 2.19 meters (bottom right). Low resistivity values in blue to green colours, high resistivity values in yellow to red and purple. Electrode distance of 0.5.

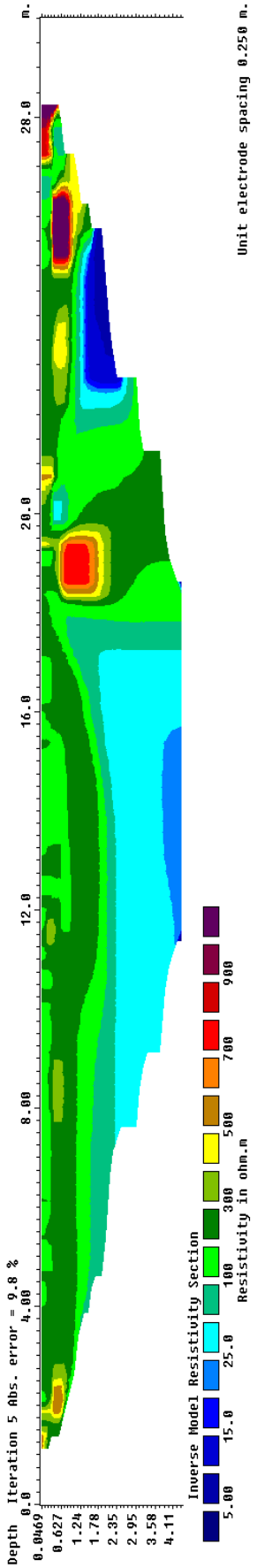

Figure 5: 2D Resistivity data of the Monastery Hill. Profile from the middle of the resistivity survey done east of the house. North to the right. Length 30 m; Depth 4.5 m. Low resistivity values in blue to green colours, high resistivity values in yellow to red and purple. Electrode distance 0.5 meter.